Revista Brasileira de Geografia Física v.18, n.02 (2025) 1523-1547.

Revista Brasileira de Geografia Física

ISSN:1984-2295

Homepage:https://periodicos.ufpe.br/revistas/rbgfe

Estimation of Offshore Wind Speed in the Coastal Region of The Southern State of Bahia

Geovanna Cruz Fernandes[1], Angelo Teixeira Lemos[2], Douglas Bitencourt Vidal[3], Ednildo Andrade Torres[4]

[1] Bacharel em Engenharia de Petróleo, Mestranda em Ciências e Tecnologias Ambientais, Universidade Federal do Sul da Bahia, Instituto Federal de Educação, Ciência e Tecnologia da Bahia, Centro de Formação em Ciências Ambientais, BR-367, Km 10, Rodovia Porto Seguro-Eunápolis, CEP 45810-000, Porto Seguro, BA, Brasil. ORCID: https://orcid.org/0000-0002-4361-8535. geovannafernandes1@hotmail.com (autor correspondente). [2]Doutor em Oceanografia Ambiental, Professor Titular, Universidade Federal do Sul da Bahia, Centro de Formação em Ciências Ambientais, Campus Sosígenes Costa, BR-367, Km 10, Rodovia Porto Seguro-Eunápolis, CEP 45810-000, Porto Seguro, BA, Brasil. ORCID: https://orcid.org/0000-0003-1229-9807. [3] Doutor em Engenharia Industrial, Universidade Federal da Bahia, Escola Politécnica/PEI, Rua Aristides Novis, n° 2, Federação CEP 40.210-630, Salvador, BA, Brasil. ORCID: https://orcid.org/0000-0002-7150-1895. bitencourt_douglas@hotmail.com. [4] Doutor em Energia, Professor Titular, Universidade Federal da Bahia, Escola Politécnica/PEI, Rua Aristides Novis, n° 2, Federação CEP 40.210-630, Salvador, BA, Brasil. ORCID: https://orcid.org/0000-0002-0574-5306.

Artigo recebido em 24/06/2024 e aceito em 01/01/2025

A B S T R A C T

Offshore wind energy has gained global prominence due to the greater intensity and consistency of maritime winds compared to terrestrial winds, which increases the efficiency of wind farms. This study aims to estimate the average offshore wind speeds in the southern coastal region of Bahia, between the municipalities of Ilhéus and Mucuri, and to validate the applicability of the WRF (Weather Research and Forecasting) model for characterizing the wind profile in the area. For this purpose, statistical analyses based on ERA5 (European Centre for Medium-Range Weather Forecasts Reanalysis v5) reanalysis data and observations from Automatic Weather Stations (EMAs) were used, employing techniques such as Pearson correlation, repeated measures ANOVA, and Taylor Diagrams. Validation indicated good agreement between the model results and observational data, with minor discrepancies. Relevant seasonal variations were observed, with stronger winds in winter, especially between latitudes 17.5°S and 18.5°S. Average wind speeds ranged from 3.5 to 4.5 m/s at 100 m and from 4.5 to 5.5 m/s at 150 m, with peaks up to 6.5 m/s. These results confirm the significant potential for offshore wind energy generation in the region at heights above 100 m. The study provides a solid technical foundation for the strategic planning of wind energy projects in the analyzed area.

Keywords: offshore wind energy, offshore wind potential, WRF atmospheric modeling, wind speed, climate reanalysis.

Estimativa da Velocidade do Vento Offshore na Região Litorânea do Sul do Estado da Bahia

R E S U M O

A energia eólica *offshore* ganhou destaque globalmente devido à maior intensidade e consistência dos ventos marítimos em comparação aos terrestres, o que eleva a eficiência dos parques eólicos. Este estudo tem como objetivos estimar as velocidades médias de vento offshore na região costeira sul da Bahia, entre os municípios de Ilhéus e Mucuri, e validar a aplicabilidade do modelo WRF (*Weather Research and Forecasting*) para a caracterização do perfil de ventos na área. Para isso, foram utilizadas análises estatísticas baseadas em dados de reanálise do ERA5 (*European Centre for Medium-Range Weather Forecasts Reanalysis v5*) e observações de Estações Meteorológicas Automáticas (EMAs), com técnicas como correlação de Pearson, ANOVA de medidas repetidas e Diagramas de Taylor. A validação indicou boa correspondência entre os resultados do modelo e os dados observacionais, com pequenas discrepâncias. Observou-se variações sazonais relevantes, com ventos mais intensos no inverno, principalmente entre as latitudes 17,5°S e 18,5°S. As velocidades médias do vento variaram de 3,5 a 4,5 m/s a 100 m de altura e de 4,5 a 5,5 m/s a 150 m, com picos de até 6,5 m/s. Esses resultados confirmam o potencial significativo para geração de energia eólica *offshore* na região a alturas superiores a 100 m. O estudo oferece uma base técnica sólida para o planejamento estratégico de projetos eólicos na área analisada.

Palavras-chave: energia eólica offshore, potencial eólico offshore, modelagem atmosférica wrf, velocidade do vento, reanálise climática.

Introduction

Offshore wind energy has emerged globally as a promising solution for diversifying energy matrices and reducing greenhouse gas emissions (Delgado & Filgueiras, 2022). Due to the lower roughness of the maritime surface, ocean winds are more intense and consistent, increasing the efficiency of offshore wind farms compared to onshore ones (Bahamonde & Litrán, 2019; Golbazi & Archer, 2020; Lange et al., 2004; Nezhad et al., 2021). These factors reinforce the relevance of this renewable energy source on a global scale.

The advancement of offshore wind technology depends on accurate assessments of wind resources conducted with the help of numerical models, such as the WRF (Weather Research and Forecasting) (Li et al., 2023; Liu et al., 2024; Saadatabadi et al., 2024). These models allow the simulation of maritime wind behavior and are widely used for short- and medium-term forecasting, as well as for analyzing future climate change scenarios (Khan & Tariq, 2018; Petersen, 2017). However, their accuracy requires the calibration of region-specific physical parameters, such as planetary boundary layer parameterization schemes and the integration of observational data (Mughal et al., 2017; Zack et al., 2010).

In Brazil, although onshore wind energy has significantly advanced, research on offshore potential remains scarce (Barroso et al., 2022; Freire & Fontgalland, 2022; Gorayeb et al., 2022). The northeastern coast, in particular, offers favorable conditions for maritime wind power generation. However, the lack of observational data offshore and uncertainties in modeling pose significant barriers to the implementation of projects in the region (Silva et al., 2017; Barthelmie et al., 2016). In the southern region of Bahia, especially between the municipalities of Ilhéus and Mucuri, the potential for offshore wind energy development is considerable. Still, the lack of regional numerical model validations and reliable observational data increases uncertainties about wind conditions.

Recent studies, such as those by Li et al. (2023) and Liu et al. (2024), have demonstrated the utility of the WRF model in simulating offshore wind conditions in various regions. However, these studies also emphasize the need for further validation of such models in topographically complex regions, like the southern coast of Bahia. These areas are characterized by specific climatic and geographical conditions that require additional calibration of physical parameters to ensure accurate predictions. Despite the advancements in offshore wind research, there remains a gap in region-specific data validation that limits the accuracy of model-based wind resource assessments, especially in regions like Bahia, where detailed and reliable observational data is lacking.

The absence of specific studies and reliable offshore data raises critical questions: how can numerical models be adequately validated to estimate wind conditions in the southern region of Bahia? Are existing models, such as WRF and ERA5, reliable enough to support strategic decisions regarding the installation of offshore wind farms? Based on these questions, the following hypothesis is proposed: the WRF model, validated with ERA5 reanalysis data and observations from automatic weather stations, can accurately estimate offshore wind conditions in the southern region of Bahia, providing a technical foundation for planning wind energy projects. This study aims to fill the gap identified in previous research by validating the WRF model for local conditions and offering insights for offshore wind project planning in Brazil.

Accordingly, this study aims to: (1) estimate the average offshore wind speeds in the region; (2) validate the WRF model using ERA5 reanalysis data and observations from Automatic Weather Stations (EMAs); and (3) provide a technical foundation for planning wind projects, contributing to the sustainable development of Brazil's energy matrix.

To achieve these objectives, the study utilized WRF model simulations with a spatial resolution of 3 km, covering the period from September 2013 to September 2014. The results were compared with ERA5 reanalysis data and local observations, enabling robust statistical analyses and cross-validations. This methodological approach aligns with recent studies on offshore wind potential, ensuring high spatial resolution to capture large- and mesoscale processes (Chancham, Waewsak & Gagnon, 2017; Pelser et al., 2024).

Methodology

The methodology of this study was based on the definition of the area of interest and the study period, as outlined in the Computational Simulation Database of the WRF model (Weather Research and Forecasting), following the approach established by De Jong et al. (2017). The study period was determined based on the availability of validated data from the responsible institutions, coinciding with the spring equinox from September 22, 2013, to September 22, 2014.

A thorough survey of available wind speed data in the delimited offshore region was conducted, using three primary sources: WRF modeling outputs, ECMWF (ERA) reanalysis, and in situ monitoring data from Automatic Weather Stations (EMA) of the National Institute of Meteorology (INMET). The ERA reanalysis data were obtained directly from ECMWF, while the in situ monitoring data, due to the limitation of offshore monitoring locations, utilized the EMA Ilhéus (A410) station, located 11 km onshore from the coast. These onshore data were carefully extrapolated to the heights of 100 m and 150 m using the logarithmic wind profile method (or specify another extrapolation method, e.g., power law or other statistical techniques), which is standard for adjusting wind measurements to standard heights for offshore wind assessment.

The wind speed data from all three sources were subjected to statistical analysis. To correlate and validate the data from these sources, the Repeated Measures ANOVA Test, Taylor Diagram, and Pearson Correlation were used, as described by Stull (2016) and Wilks (2020). These methods were employed to assess the consistency between the model outputs and observational data, as well as to detect any significant differences in wind speeds across datasets.

After the data validation, the WRF model outputs were processed to generate seasonal (by season) and annual graphical representations of the study period, thus providing a detailed estimate of offshore wind speed for the study area. These graphical outputs allowed for the identification of seasonal variations and a more accurate representation of wind conditions over the study period.

Additionally, validation metrics such as Root Mean Square Error (RMSE) and bias were used to assess the accuracy of the WRF model simulations, comparing the predicted wind speeds with the observed data from both in situ stations and ERA5 reanalysis data.

Characterization of the study area

The Northeast region of Brazil is particularly favorable for studies on the potential for offshore wind energy generation, owing to its ideal geographical characteristics for this type of exploration (Rabelo et al., 2023). The region's extensive coastline features shallow waters and gently sloping seabeds, which not only facilitate the anchoring of offshore wind structures but also maximize the potential for wind energy capture (Vinhoza & Schaeffer, 2021). Furthermore, studies have indicated favorable wind consistency and intensity along the coast, suggesting a high potential for stable offshore wind energy production (CEPEL, 2017).

The study area defined for this research focuses on the coastal zone of the southern state of Bahia, specifically within the Exclusive Economic Zone (EEZ), extending up to 24 nautical miles (44.4 km) from the coast, with a latitude range between 14.5ºS and 18.4ºS. This area was delineated using the Baseline of Brazilian territory and the 24-mile line as defined by the Brazilian Navy (Marinha do Brasil, 2024), as shown in Figure 1.

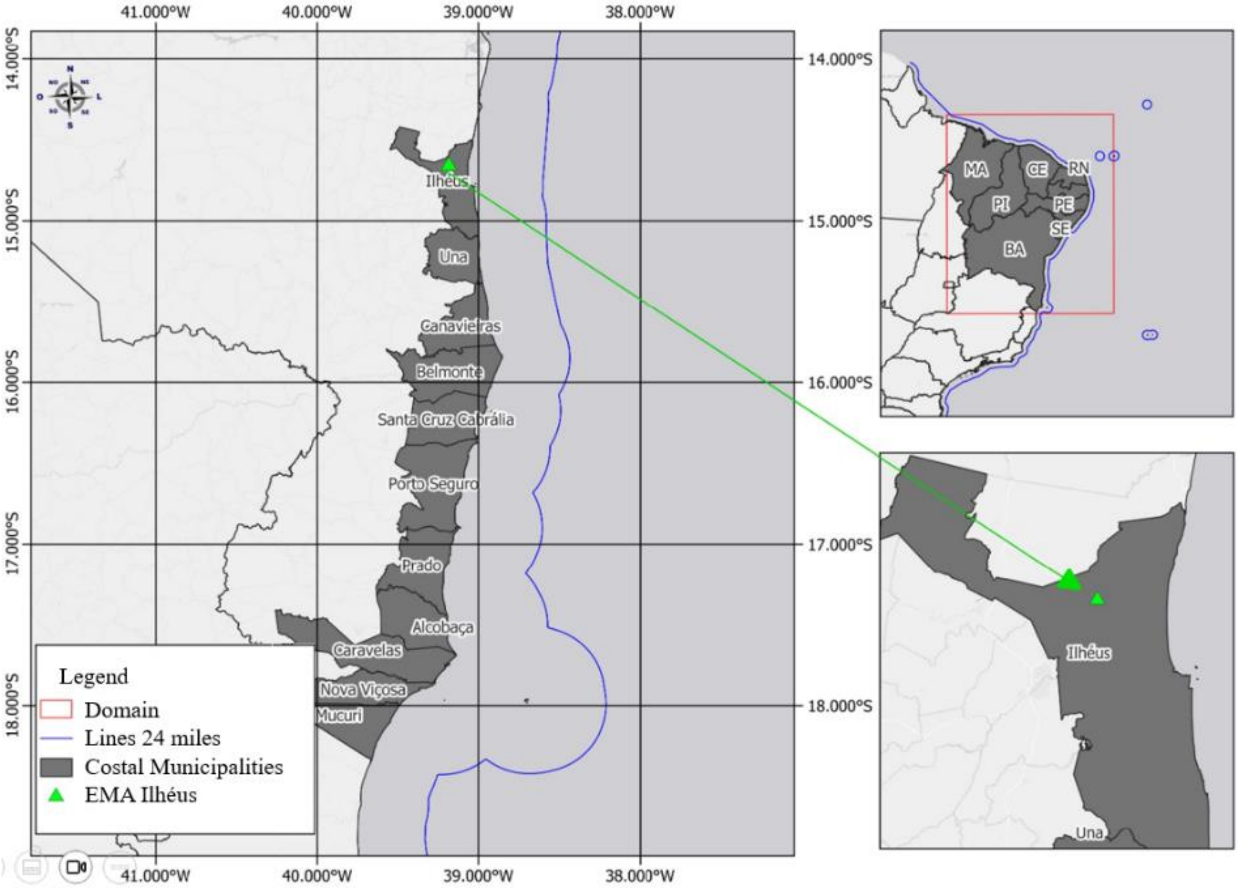

Figure 1 - Delimitation of the study area.

The data sources considered in this methodology include in situ monitoring by INMET, the ERA reanalysis database, and WRF computational modeling. The wind speed data collection period was determined to span from September 22, 2013, to September 22, 2014, which coincides with the spring equinox, based on the availability of validated data from the responsible institutions for each data source. These timeframes were chosen to align with periods of validated data availability, ensuring the reliability of the study results.

Data used

In situ wind data

The Northeast region of Brazil has limited data sources for analyzing wind speed in offshore regions (Santana et al., 2020; Santana & Silva, 2020). There are no available offshore wind speed measurement data for the study area, so onshore measurement data from the nearest Automatic Weather Stations (EMA) were used for statistical validation (Coriolano et al., 2022; Kovalski, 2023; Nascimento et al., 2022; Santos, 2020). The data from Anemometric Towers (ATs) were provided by projects managed by the National Institute of Meteorology (INMET) (https://mapas.inmet.gov.br/).

Despite the presence of several EMAs in the study area, only the Ilhéus EMA provided hourly measurement data for the entire study period. The EMA Ilhéus is located at the geographic coordinates 14°39'32"S and 39°10'53"W, and has been operational and providing validated data since January 24, 2003. The wind speed measurements were collected at a height of 10 m.

The raw data collected by the EMA were available on an hourly basis and were processed and organized using Microsoft Excel. Any records that showed discrepancies or wind speeds below 0.1 m/s were discarded due to potential equipment precision issues or recording failures. To calculate the hourly averages, all measurements recorded at the same specific hour of the day were grouped. For example, all wind speed measurements recorded at 00:00 were grouped to calculate the corresponding average for that hour, and this same procedure was repeated for every hour from 01:00 to 23:00.

By calculating the averages for each hour, we obtained the mean wind speed for each hour of the day during the analyzed period. These hourly averages were then subjected to trend line analysis and standard deviation analysis to identify patterns in the wind data. Finally, the data were extrapolated to the heights of interest (100 m and 150 m) using the logarithmic wind profile method (or specify another method used, e.g., power law), to adjust the measurements to the standard heights required for offshore wind analysis.

ERA5 Reanalysis data

Reanalysis data are produced by integrating numerical forecasts with observational data from the global meteorological network. The European Centre for Medium-Range Weather Forecasts (ECMWF) developed the ECMWF Reanalysis v5 (ERA5), which is the fifth generation of global climate reanalysis produced by the Copernicus Climate Change Service and implemented by Hersbach et al. (2020).

ERA5 was created using four-dimensional data assimilation of the atmosphere and surface data through the ECMWF Integrated Forecast System (IFS). This system operates with 137 vertical levels in sigma coordinates, which use surface atmospheric pressure as a reference. Additionally, ERA5 provides a horizontal spatial resolution of 31 km for all atmospheric levels. The dataset spans from January 1950 to the present, offering hourly estimates of a wide range of atmospheric, terrestrial, and oceanic climate variables. ERA5 also provides uncertainty information for all these variables, although at reduced spatial and temporal resolutions (Tian et al., 2023; Wang et al., 2023; Shi et al., 2024).

Hourly wind speed data at 100 m were available for the same period as the observational data, enabling a comparative and statistically significant analysis (Varga & Breuer, 2022). The geographical region selected for this analysis includes both the study area and the Ilhéus weather station.

The pre-processing of the ERA5 data involved temporal interpolation to adjust the resolution of the observed in situ data from EMA Ilhéus. Temporal interpolation was necessary because while ERA5 provides wind speed records for all hours and days of the studied period, the EMA Ilhéus data have gaps due to maintenance periods or equipment malfunctions. Therefore, the available data from EMA Ilhéus were compared only to ERA5 data for those specific hours when EMA Ilhéus data were available, excluding ERA5 measurements where no corresponding EMA measurements existed.

To ensure a consistent comparison between the datasets, hourly averages of the wind speed data were calculated for both ERA5 and EMA Ilhéus. This process ensured that the temporal resolution of the data was aligned, allowing for meaningful statistical analysis. The temporal interpolation of ERA5 data helped fill the gaps in EMA Ilhéus data, making the comparison between the two datasets more robust and statistically significant.

WRF mesoscale numerical prediction modeling

The mesoscale model used in this study was WRF version 4.2, developed by the National Center for Atmospheric Research (NCAR). From a computational perspective, a single domain configuration is more efficient, according to the structure of the WRF model code, which is designed to resolve atmospheric dynamics in domains with larger grid points (Kruse et al., 2013; Moreno et al., 2020). This approach optimizes computational performance while ensuring high accuracy in simulating atmospheric conditions.

WRF (Weather Research and Forecasting) is an atmospheric dynamic modeling system widely used in both meteorological research and operational environments. It numerically resolves a wide range of atmospheric processes within the atmospheric boundary layer, including the effects of surface roughness (both onshore and offshore), heat and moisture fluxes, atmospheric stability, wind speed profiles, and turbulence. The WRF simulations and atmospheric dynamics calculations are based on a comprehensive set of physical processes, including microphysics, convection, turbulence, surface processes, boundary layer processes, and radiation (Loriato et al., 2018).

For this study, the WRF model was configured with a comprehensive set of physical parameterizations to optimize its performance in atmospheric simulations. These configurations include the planetary boundary layer (PBL) scheme, surface scheme (CP), soil model (MS), cloud microphysics, cumulus parameterization, and radiation processes. This set of configurations is designed to capture complex weather dynamics, especially for simulations that require sensitive initial and boundary conditions in the study areas (Gonçalves et al., 2024; Yu et al., 2022).

For the offshore wind study, a 3 km resolution grid was adopted to compare the WRF simulations with observed wind resource data over the Atlantic Ocean near the coast of Northeast Brazil, from the east coast of Bahia to parts of the state of Maranhão. The grid extension was chosen to capture the effects of mesoscale weather conditions on the offshore wind resource, allowing the model to develop regional circulations driven by the physical processes occurring in the area (Silveira & Carvalho, 2021; Wu et al., 2022). This resolution enables the model to resolve local-scale phenomena that significantly impact wind energy production.

The domain determination for simulating offshore wind resources in Northeast Brazil was based on the research of De Jong et al. (2017) and Dörenkämper et al. (2020). The wind speed data simulation was configured at heights of 100 m and 150 m, with hourly data collected over a period of 386 days. This period was chosen to capture seasonal and daily variations in wind speed, which are critical for assessing wind energy potential.

For the selection of the physical parameters, we relied on research from previous offshore studies that demonstrated satisfactory results for simulating the meteorological variable wind speed. These studies provided evidence that the chosen parameterizations performed well in offshore environments and were effective in simulating wind speed at the required heights (Gonzáles-Mingueza & Muñoz-Gutiérrez, 2014; Lumbreras & Ramos, 2013; Miglietta, Zecchetto & De Biasio, 2013). Table 1 describes the initial configuration for the physical parameterization used in the WRF model simulation.

Table 1 - Configurations and physical parameterizations used in the WRF model simulation.

Parameter	**Value/Description**
Mesoscale model	WRF
Horizontal resolution of mesoscale model	3 km
Wind data base	ERA5 for the period 09/2013 to 09/2014
Topography data base	SRTM with 30 m spatial resolution
Roughness data base	MODIS sensor with 925 m spatial resolution
Number of vertical atmospheric levels	61
Shortwave and longwave radiation	Rapid Radiative Transfer Model (RRTMG)
Microphysics	WRF Single-Moment 6-class
Cumulus	Kain-Fritsch
Surface layer	MYJ
Land surface model	Noah Land Surface Model (Noah LSM)
Planetary boundary layer	MYNN 2.5

Trend Analysis and Extrapolation of Vertical Wind Speed

Trend Analysis

Trend analysis involves several important methodological steps aimed at determining the direction and significance of variations in data over time. The primary objective is to identify whether there is an increasing or decreasing trend in the data, which can provide valuable insights for future predictions and decision-making.

To model the trend, regression methods are applied, typically using simple linear regression. In this context, the observed value is treated as the dependent variable (Y), while time (X) serves as the independent variable. The relationship between time and wind speed can be described by the following linear equation:

$$Y = \beta 0 + \beta 1X + \epsilon$$

Where $\beta 0$ represents the intercept, which is the estimated value of Y when X equals 0, $\beta 1$ is the slope coefficient, which indicates the rate of change of Y with respect to X (i.e., the trend) and ϵ denotes the residual error, representing the difference between the observed and predicted values.

Once the model is set up, the next step is to estimate the slope coefficient ($\beta 1$) using least squares methods. This approach minimizes the sum of the squared differences between the observed values and the predicted values (based on the model), thus providing the best estimate of the relationship between time and wind speed.

The slope coefficient ($\beta 1$) indicates the direction of the trend: a positive slope ($\beta 1 > 0$) suggests an increasing trend, indicating that wind speeds are rising over time. A negative slope ($\beta 1 < 0$) suggests a decreasing trend, indicating that wind speeds are declining.

After calculating the slope, the T-Test is performed to assess the statistical significance of the slope coefficient. The hypothesis test is formulated as follows: H0: $\beta 1 = 0$ (no trend); Ha: $\beta 1 \neq 0$ (there is a trend).

The T-Test is calculated using the following formula:

$$T = \frac{\beta 1}{SE(\beta 1)}$$

Where SE(β1) is the standard error of the slope coefficient estimate, which measures the variability of the estimated slope.

Next, the P-value is calculated, which represents the probability of observing a slope as extreme as the estimated value, assuming the null hypothesis (H0) is true. The P-value helps to determine whether the slope is statistically significant: if the P-value is less than the significance level (α) (usually 0.05), we reject H0 and conclude that there is a statistically significant trend. If the P-value is greater than α, we fail to reject H0, indicating that the data do not show a significant trend.

This process enables the identification of whether the data exhibit a trend over time, and it provides a foundation for future analyses and informed decision-making.

Extrapolation

In wind energy studies, current interest is primarily focused on wind speeds at the rotor height of wind turbines, which typically ranges from 80 to 150 m (Alayat, Kassem, & Çamur, 2018; Mathos et al., 2020). However, available observational data are often collected at low-altitude anemometers, and there is even less data available in offshore zones, where measurements are typically made through ocean buoys, ships, and other floating platforms. Therefore, it becomes necessary to extrapolate the vertical wind speed, which estimates the wind speed at higher altitudes based on measurements taken at reference heights at lower altitudes (Crippa et al., 2021; Kent et al., 2018).

The logarithmic law is commonly used for this type of extrapolation, based on the wind speed measured at the reference height and the terrain roughness factor (Bañuelos-Ruedas, Angeles-Camacho, & Ríos-Marcuello, 2010). This method is effective for predicting wind speeds at higher altitudes, especially in offshore environments, where direct measurement at those heights is often impractical.

To standardize the results and facilitate statistical comparisons across different data sources, it was necessary to extrapolate the wind speed values to the heights of interest for this study. The equation that describes the wind speed at the rotor height of the wind turbine is as follows:

$$U = U_{ref}\,\frac{ln\,(\frac{h}{z_0})}{ln\left(\frac{h_{ref}}{z_0}\right)}$$

In this formula, U is the wind speed at the desired height h (in m/s), while Uref is the wind speed measured at the reference height $h$ref (in m/s). The height h is the height at which the wind speed is to be calculated, and $h$ref is the reference height where the wind speed was originally measured. In this research, a neutral atmosphere with roughness z0 = 0.0002 m was assumed, a value considered appropriate for calm sea conditions (Li et al., 2020; Machrafi, 2012; Wieringa, 1986).

To estimate the wind speed at heights ideal for wind power generation, vertical extrapolation was performed to the heights of 100 m and 150 m. Wind speed data obtained from EMA Ilhéus, measured at a height of 10 m, were extrapolated to the target heights of 100 m and 150 m using the logarithmic law. The ERA5 data, which were already available at a height of 100 m, were extrapolated only to 150 m. For the WRF model, vertical extrapolation was not required, as the model automatically performs vertical interpolation during the data processing to extract information at various heights within the model's grid.

Statistical Comparison

To ensure compatibility between the data from the three different sources, temporal and spatial interpolation were applied to normalize the wind speed values. The wind speeds were then organized to present the average wind speed for each hour of the day, for each of the three data sources: in situ monitoring (INMET data), WRF (weather prediction model), and ERA (global reanalysis from ECMWF). This step ensured that the data from the different sources were comparable and aligned in both temporal and spatial resolution.

The correlation between the wind speeds from these three sources was evaluated using Pearson's correlation coefficient. This method provides a measure of the strength and direction of the linear relationship between the wind speeds from different sources. A high correlation indicates that the wind speed data from the sources are consistent with each other, while a low correlation suggests discrepancies between the datasets.

To analyze whether there were significant statistical differences between the wind speeds observed by the three sources, repeated measures ANOVA was applied. This test is appropriate for data where the same subject (in this case, the study area) is measured multiple times under different conditions (i.e., using different data sources). The ANOVA helps determine if the observed differences in wind speed between sources are statistically significant. Specifically, the null hypothesis (H0) posits that there are no significant differences between the sources, while the alternative hypothesis (Ha) suggests that there are significant differences.

Additionally, the Taylor Diagram was used for a comprehensive assessment of the wind speed data. The Taylor Diagram allows the simultaneous visualization of multiple statistical metrics, including correlation, standard deviation, and root mean square error (RMSE), providing a holistic evaluation of the model's performance. The correlation indicates how well the simulated data matches the observed data, while the standard deviation and RMSE provide measures of the variability and overall error in the simulation, respectively.

The validation of the results compared the simulated wind speed data from the WRF model with the observed data from the EMA (in situ) and ERA5 (reanalysis). This comparison allowed for the assessment of the accuracy of the WRF model, helping to determine how well the model's predictions align with actual wind speed measurements and ensuring the reliability of the model for future wind energy predictions.

Pearson Correlation

The Pearson correlation coefficient (r) is a widely used statistical measure that quantifies the strength and direction of the linear relationship between two variables. In this study, Pearson's correlation was used to assess the relationship between wind speeds obtained from three distinct sources: in situ monitoring (INMET data), the WRF weather prediction model, and ERA5 global reanalysis from ECMWF. The Pearson correlation coefficient ranges from -1 to 1, where: 1 indicates a perfect positive correlation (i.e., as one variable increases, the other also increases proportionally), 0 indicates no linear correlation (i.e., the two variables are not linearly related), -1 indicates a perfect negative correlation (i.e., as one variable increases, the other decreases proportionally) (Benesty et al., 2009; Xiang et al., 2022).

Mathematically, Pearson's correlation is calculated using the following formula:

$$r = \frac{\sum_{i=1}^{n}(x_i - \bar{x})(y_i - \bar{y})}{\sqrt{\sum_{i=1}^{n}(x_i - \bar{x})^2 \sum_{i=1}^{n}(y_i - \bar{y})^2}}$$

Where:

- x_i and y_i are the values of the two variables for which we are calculating the correlation;
- $\bar{x}$ and $\bar{y}$ are the means of the x and y values, respectively;
- n is the number of value pairs being considered.

In this study, the Pearson correlation coefficient was used to determine the degree of agreement between different wind speed data sources, including the in situ monitoring data (INMET), the WRF model simulations, and the ERA5 reanalysis data. The correlation coefficient indicates how strongly the wind speed values from the different sources are linearly related, providing insight into the accuracy and consistency of the model's predictions.

By calculating the Pearson correlation, the study evaluates whether the WRF model's predictions align with observed wind speeds and reanalyzed data, thus validating the model's ability to replicate real-world conditions. A high positive correlation (close to 1) would indicate that the simulated and observed data are in strong agreement, whereas a low or negative correlation would suggest discrepancies, pointing to potential areas for model improvement.

This analysis plays a crucial role in assessing the reliability of the WRF model for wind energy studies, helping to confirm whether the model is capable of accurately predicting wind speeds in the study region, as compared to observed and reanalyzed data sources (Benesty et al., 2009; Xiang et al., 2022).

Repeated Measures ANOVA Test

The repeated measures ANOVA test is a statistical technique used to compare the means of three or more groups where the same samples are measured multiple times under different conditions or at different times. This method is particularly useful in longitudinal or time series studies, where the observations are correlated due to repeated measurements on the same subjects over time. The test is applied to evaluate significant variations in wind speeds collected at different hours over the course of a year, considering the correlation between repeated hourly measurements. This approach allows for the detection of temporal patterns and variations influenced by seasonal or diurnal factors, helping to better understand the dynamics of wind speed under different temporal conditions (Langenberg et al., 2022; Maslor & Hasan, 2024).

The statistical model for the repeated measures ANOVA can be expressed as:

$$Y_{ijkl} = \mu + D_j + T_k + e_{ijk}$$

Where:

- Y_{ijkl} is the wind speed observed at time i of the day j;
- μ is the overall average of the wind speed;
- D_j is the effect of time of day i (factor of repeated measures);
- T_k is the effect of subject j (in this case, the "subject" can be interpreted as the day of the year, as measurements are taken repeatedly over the course of the days);
- e_{ijk} is the residual error associated with the observation at time i of day j.

The repeated measures ANOVA decomposes the total variation of the observations into components attributed to the different factors, such as time of day and day of the year, and their interactions. This decomposition helps assess whether the variation in wind speed is significant between different times of the day, days, or seasons, and if the temporal effects (e.g., diurnal or seasonal) have a statistically significant impact on wind speed variation.

To ensure that the model is valid, the residuals (i.e., the difference between the observed and predicted values) must meet several assumptions: normality: The residuals should follow a normal distribution; homoscedasticity: The variance of the residuals should be constant across different levels of the independent variables (time of day and day of the year); independence: The residuals should be independent of each other, meaning the measurement errors are not correlated. These assumptions are verified through graphical methods (e.g., residual plots) and appropriate statistical tests (Muhammad, 2023).

Taylor Diagram

The Taylor diagram is a graphical tool used to compare forecast data sets (f_n) with reference data (r_n) by visualizing statistical metrics such as Root Mean Square Error (RMSE), Standard Deviation, and Pearson Correlation Coefficient. Each dataset is represented as a point on the diagram, with the position of the point determined by these three statistics. Closer points indicate a higher degree of similarity between the datasets, while distant points suggest greater discrepancies (Tuchtenhagen, 2019).

The RMSE measures the accuracy of numerical results by expressing the error in the same units as the variable being analyzed. It quantifies the difference between the model output and the observed value, considering magnitude, frequency, and phase. However, RMSE is not influenced by systematic errors. It serves as an indicator of the overall disagreement between the model predictions and observations (Willmott, Matsuura, & Robeson, 2009).

The formula for RMSE is:

$$RMSE = \frac{\sum_{i=1}^{n}(r_n - f_n)^2}{n}$$

Where:

- r_n represents the observed wind speed,
- f_n represents the forecasted wind speed,
- n is the total number of data points.

A smaller RMSE indicates a better fit between the model predictions and the observed data, while a larger RMSE indicates greater discrepancies.

When the ratio between the model's standard deviation and the standard deviation of the observations exceeds one, it suggests that the model overestimates the amplitude of variations in the observed data (Coles, 2001).

The Pearson correlation coefficient (r) measures the linear relationship between two quantitative variables. It indicates the model's ability to reproduce the frequency and phase structure of the observed data. The values of r range from -1.0 to 1.0, where:

- 1 indicates a perfect positive correlation (the model perfectly matches the observations),
- -1 indicates a perfect negative correlation (the model completely opposes the observations),
- 0 indicates no linear correlation (the model is unrelated to the observations).

It is important to note that a zero correlation does not rule out the possibility of a non-linear relationship, which should be explored using alternative methods (Wilks, 2020).

The Pearson correlation is computed as:

$$R = \frac{\frac{1}{n}\sum_{1}^{N}(f_n - {}'f)(r_n - {}'r)}{\sigma_f \, \sigma_r}$$

Where:

- ‘f and ‘r are the mean values of the forecasted and observed wind speeds,
- σ_f and σ_r are the standard deviations of the forecasted and observed data.

The relationship between the statistics—correlation, RMSE, and standard deviation—is represented geometrically by the law of cosines. In the Taylor diagram, each dataset is represented by a point, determined by the values of these three statistics. The closeness of the points reflects the similarity between the datasets: the closer the points, the greater the similarity. This diagram provides a powerful way to assess how well the model reproduces the observed data in terms of both magnitude and temporal structure.

According to Tuchtenhagen (2019), the diagram is particularly useful for selecting the best model representation, considering the error limits within which the real value should lie. In experimental conditions, multiple repeated measures can be taken, and the best representation of the data should be selected based on these analyses.

Presentation of WRF Model Wind Speed Data

The WRF wind speed data were processed and grouped into hourly averages, which were then organized into seasonal (by season) and annual periods for heights of 100 m and 150 m. This organization facilitated the analysis of the data from different perspectives, allowing for a more detailed evaluation of wind speed variation over time.

The seasonal grouping divided the study period into the following seasons: Spring, Summer, Autumn, and Winter. Each season was analyzed separately to observe seasonal trends and variations in wind speed. The annual grouping considered the entire study period, providing a comprehensive overview of the wind speed dynamics over the year. Separate groupings were made for each of the heights studied (100 m and 150 m).

To visualize the trends, data visualization tools were employed to graphically present the time series of the wind speed data. These tools allowed the evolution of the average wind speed on an hourly basis over time to be shown for each grouping. The visualization enabled a clearer understanding of how wind speed varied within each season and throughout the year, providing valuable insights into the temporal dynamics of the wind resource.

Results and discussions

Analysis of Wind Speeds for Each Data Source

The results of height extrapolation, reanalysis, and modeling were organized according to the predefined heights of interest for this study, allowing visualization of the wind speed in the specified area and period for the geographical location of the EMA Ilhéus.

EMA Ilhéus Observations

The data, organized in an Excel spreadsheet for further analysis, covered the study period. If all hourly measurements had been taken, there would be 8784 measurements (366 days). However, the actual number was less than expected, with 8749 measurements. These measurements were organized into hourly information for which the average for each hour of the day was calculated.

Table 2 presents the trend analysis results for the EMA Ilhéus location. The data include the slope, T-test value, and P-value.

Table 2 - Result of Trend Analysis.

Locality	**Inclination (*Slope*)**	**T-Test**	**P-value**
EMA of Ilhéus	0,0012	0,125	0,903

The application of Linear Regression to the data collected in situ allowed the identification of trends over time or in relation to other variables, providing a better understanding of the characteristics and behaviors of wind speed.

The results of the trend analysis for the locality of Ilhéus are summarized in Figure 2.

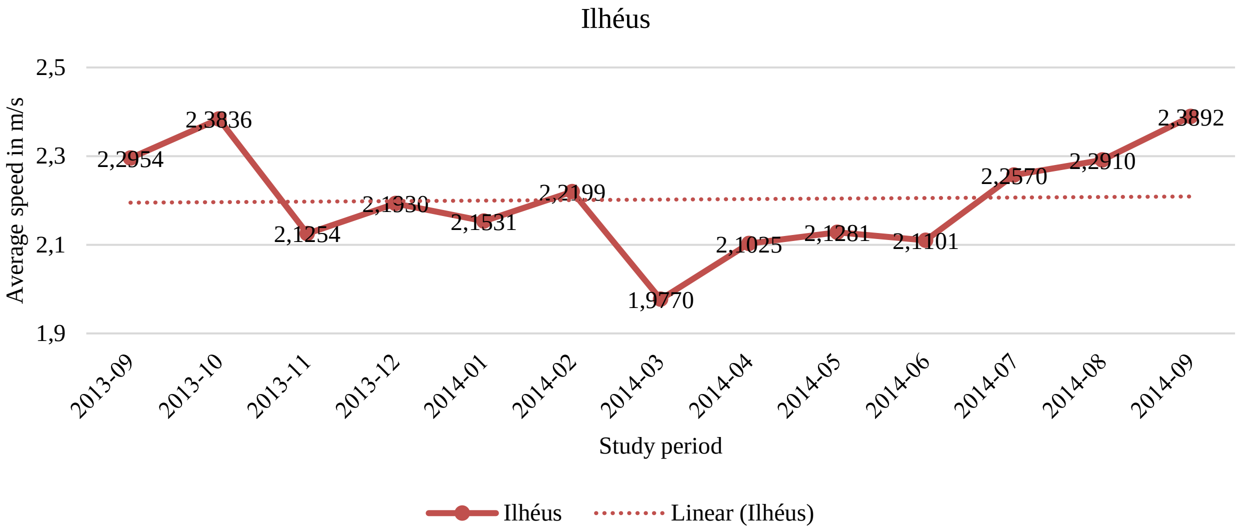

Figure 1 - Linear Regression Trend Line for Ilhéus/BA.

The slope of the linear regression is 0.0012, indicating a slight upward trend in wind speed over time. The T-test resulted in 0.125, and the p-value was 0.903, suggesting that the trend is not statistically significant, meaning there is no evidence that wind speed in Ilhéus is changing significantly over time. This suggests that the collected data are consistent and maintain a stable pattern, which is essential for long-term trend analysis.

Using data provided by the publicly accessible INMET site, it was possible to observe wind speed for the Ilhéus location at stations with anemometers at 10 m altitude. These speeds were extrapolated to heights of 100 and 150 m.

Figure 3 presents the wind speed data observed in Ilhéus by INMET. The average daily wind speed was 2.18 m/s at 10 m, 2.78 m/s at 100 m, and 2.88 m/s at 150 m. The graph shows a diurnal pattern, with wind speed increasing from 11:00 AM and peaking between 3:00 PM and 5:00 PM, with maximum values of approximately 4.5 m/s to 5.5 m/s. The speed gradually decreases during the night. This pattern is consistent across all heights, with higher speeds at elevated altitudes.

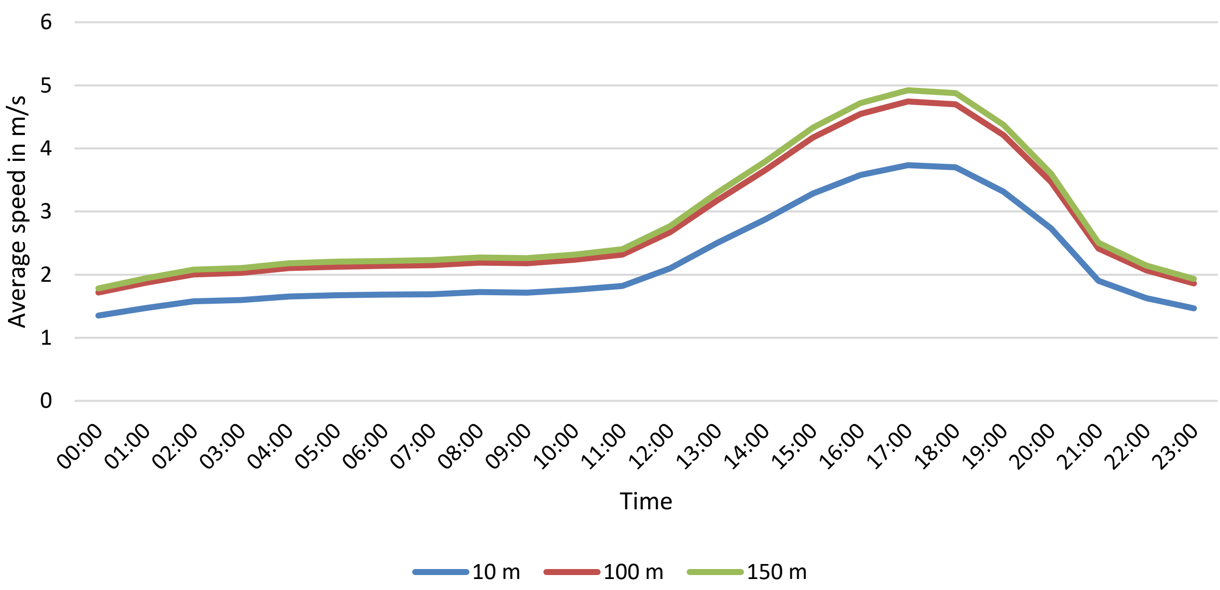

Figure 2 - Observed and extrapolated average hourly speed.

ERA5 Reanalysis Data

The hourly reanalysis data from ERA5 were used in this research to analyze the wind speed at 100 m, extrapolating it to 150 m altitude. These data cover the same period as the observational data obtained from the EMA Ilhéus.

Figure 4 presents the comparison between the hourly average wind speed simulated by ERA5 and the observational data for the altitudes of 100 m (OBS. 100 m) and 150 m (OBS. 150 m). The observed speeds show a similar behavior throughout the day, with a decrease during the first few hours and a minimum value around 04:00 hours, followed by a gradual increase until reaching a maximum peak between 13:00 and 15:00 hours, with velocities of approximately 4.5 m/s at 100 m and 5.5 m/s at 150 m. Compared to the ERA5 simulations, it is possible to notice that the simulated velocities at 100 m (ERA 100 m) closely follow the observations, although they are underestimated during the early afternoon, with a maximum value of approximately 3.5 m/s.

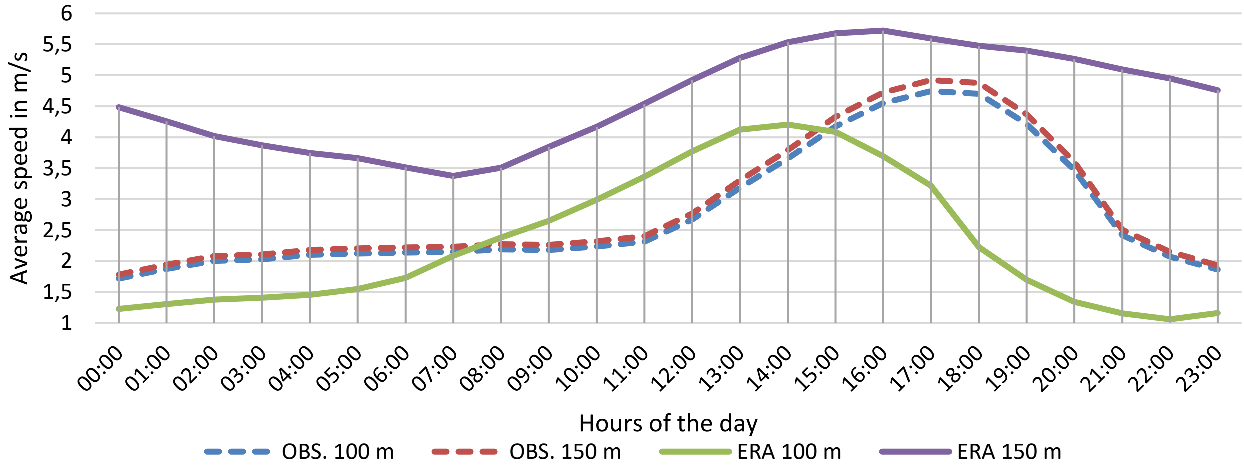

Figure 3 - Hourly Average Speed Simulated by ERA 5 Compared to Observed Results for EMA Ilhéus.

On the other hand, the simulations at 150 m (ERA 150 m) show greater precision, with values closer to those observed, especially in the period between 13:00 and 15:00 hours, indicating a peak wind speed similar to that of the observations.

The coincidence of peak wind speed times in the observations and simulations suggests that the reanalysis of ERA5 has adequate precision in representing the diurnal pattern of wind speed in Ilhéus. This is crucial for applications in wind planning, meteorology, and other areas that rely on accurate modeling of wind behavior. Despite some occasional discrepancies, ERA5 captures the main characteristics of diurnal wind variation, reflecting local meteorological factors. These results corroborate the use of ERA5 reanalysis data as a valuable tool to complement and validate observational data, offering a comprehensive overview of wind conditions in the Ilhéus region.

WRF Model Data

The use of WRF allows for accurate simulation of local anemometric conditions, taking into account surface variables and atmospheric physical processes. WRF data were simulated at one-hour intervals, covering altitudes of 100 and 150 m.

The WRF simulations indicate, through Figure 5, a more stable wind speed, between 3.4 m/s and 5 m/s at 100 m and between 3.5 m/s and 5 m/s at 150 m, reproducing the diurnal cycle with milder variations.

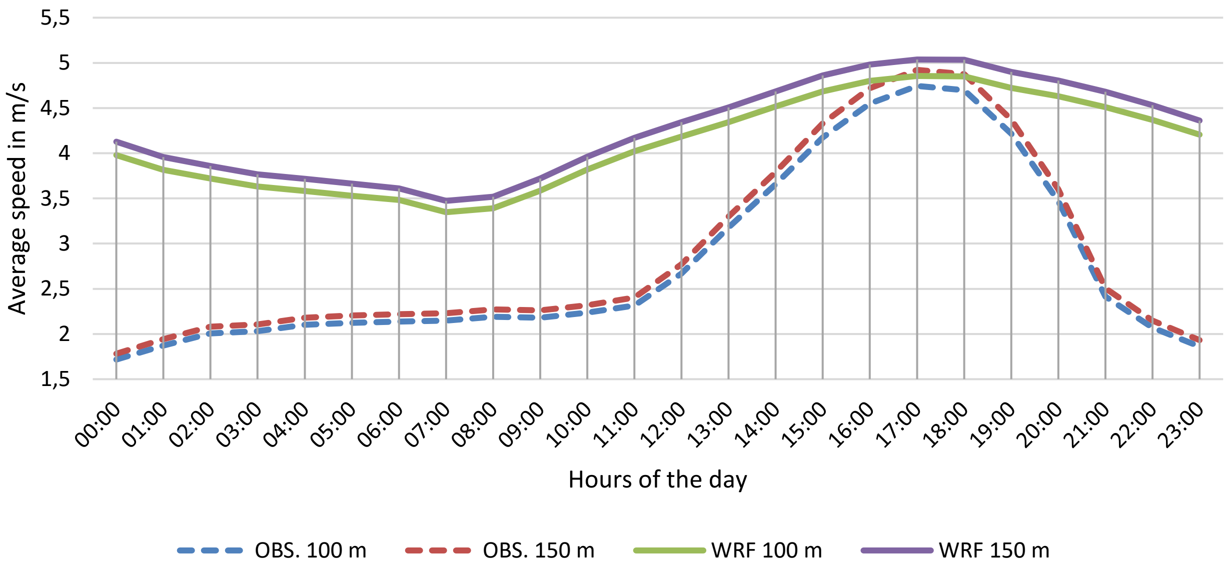

Figure 4 - Hourly Average Speed Simulated by WRF Compared to Observed Results for EMA Ilhéus/BA.

Comparisons show that the WRF tends to underestimate wind speed, especially between 1:00 PM and 9:00 PM, and reflects less of the difference in speed between 100 m and 150 m observed in the actual data.

Speeds per Source for Heights of Interest

Analyzing wind speed data from disparate sources on a single graph is important because it allows for a clear and direct comparison between actual observations and model simulations. This makes it easier to identify discrepancies and assess the accuracy and reliability of simulation models (Brower, 2012; Kaiser-Weiss et al., 2015; Piasecki, Jurasz, & Kies, 2019; Sheridan et al., 2022).

Figures 6 and 7 show the average hourly wind speed at 100 m and 150 m height, respectively, comparing observational data (OBS) with the simulations of the WRF and ERA5 models for the EMA Ilhéus locality.

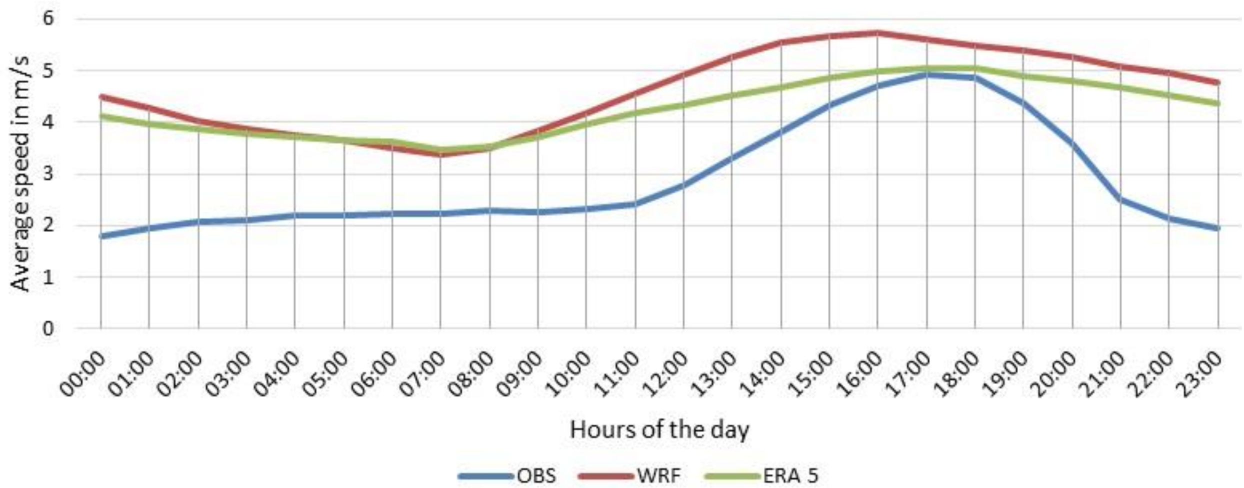

Figure 6 - Hourly Average Speed at 100 m.

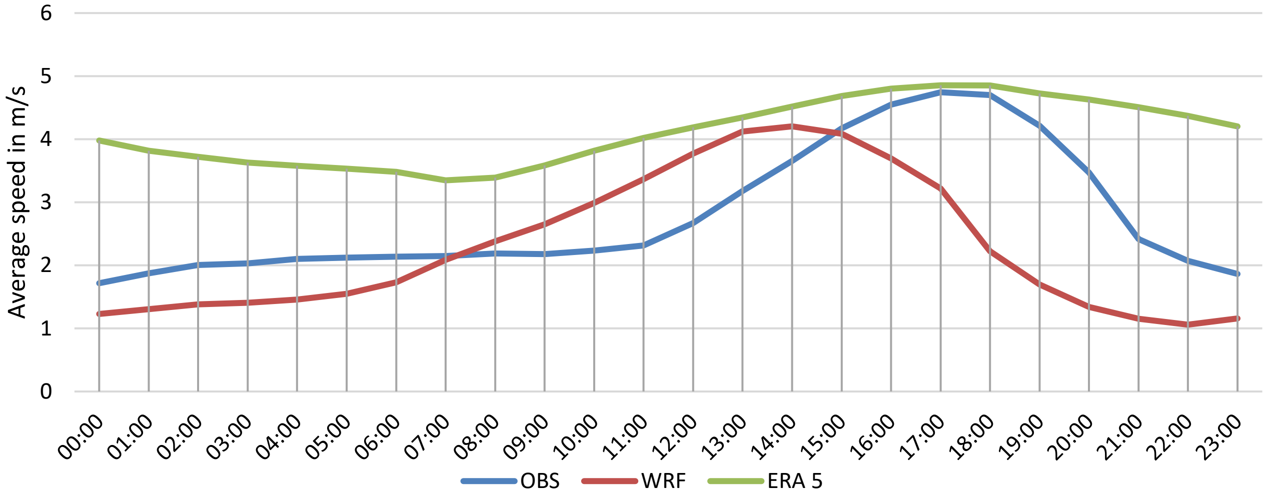

Figure 7 - Hourly Average Speed at 150 m.

In Figure 6, it can be observed that the hourly average wind speed simulated by ERA5 maintains a consistent pattern throughout the day, with a peak between 2:00 PM and 3:00 PM. However, the actual observations (OBS) show a different pattern, with a sharper increase in the early afternoon and a more pronounced peak around 3:00 PM, followed by a steep decline. The WRF model, on the other hand, shows a significant underestimation in the early hours and an overestimation during the afternoon, suggesting a temporal phase shift in relation to the observations.

Figure 7 presents the hourly average wind speed at 150 m, where it is possible to observe that both ERA5 and WRF show greater accuracy in relation to the observations (OBS), especially during the afternoon period. The WRF model, in particular, demonstrates a wind speed peak more aligned with the observations, although with slightly higher intensity. ERA5, however, maintains consistency throughout the day but slightly underestimates the maximum peak observed around 3:00 PM.

The comparison of the WRF and ERA5 model simulations with the observational data reveals important differences in the representation of the diurnal wind speed pattern. The observed discrepancies can be attributed to various factors, including model resolution, physical process parameterization, and the influence of local terrain characteristics.

According to Brower (2012), Stoevesandt et al. (2022) and Letcher (2023), accuracy in wind modeling is essential for the planning and development of wind projects, as it directly influences the estimation of energy production and the economic feasibility of the projects. Similarly, Daley (1991) points out that validating models against observational data is a fundamental step to ensure the reliability of weather forecasts.

The detailed analysis of the figures shows that, despite some occasional discrepancies, the ERA5 and WRF models are able to capture the main characteristics of the diurnal wind variation, reflecting the influence of local meteorological factors. However, the underestimation or overestimation of wind speeds at certain times of the day suggests the need for adjustments to the models to better represent local conditions.

Statistical Comparison

Repeated Measures ANOVA Test

The application of the Repeated Measures ANOVA model to wind speed data collected in situ allows the identification of trends related to the effects of time and group. This analysis determines how wind speed varies over time, highlighting statistically significant increases or decreases. In addition, it considers the impact of different groups or conditions, such as diverse localities or heights (100m and 150m), providing a detailed understanding of spatial and contextual variations in wind speed.

Table 3 presents the statistical analysis results comparing observed data with ERA and WRF datasets for Ilhéus at 100m and 150m altitudes. Key descriptive statistics and p-values highlight the variability and significance of the differences across datasets and locations.

Table 3 - Results of the ANOVA test for the studied location.

		Mean	Median	Standard Deviation	CV	Min	Max	N	IC	P-value
Ilhéus 100m	Observed	2,792	2,414	1,528	55%	0,127	9,401	8.749	0,032	
	ERA	4,105	4,127	1,475	36%	0,171	10,185	8.749	0,031	<0,001
	WRF	2,301	1,735	1,700	74%	0,033	8,031	8.749	0,036	
Ilhéus 150m	Observed	2,897	2,504	1,586	55%	0,132	9,753	8.749	0,033	
	ERA	4,259	4,282	1,531	36%	0,178	10,566	8.749	0,032	<0,001
	WRF	4,609	4,755	1,775	39%	0,054	13,455	8.749	0,037	

As shown in Table 3, both at 100m and 150m, the observed data have a coefficient of variation (CV) of 55%, indicating a significant variation in wind speed. Compared to the ERA5 and WRF data, the CV for ERA5 is 36%, while for WRF it is 74% at 100m and 39% at 150m. These results reveal a higher variability in the WRF data at 100m. The p-values (<0.001) indicate statistically significant differences between the observed values and those projected by the models.

Taylor Diagram

Taylor diagrams provide a detailed view of the performance of simulation models compared to observational data, encompassing standard deviation, correlation, and root mean square error (RMSE). Thus, the Taylor Diagram allows a quantitative assessment of the model's ability to reproduce the spatial and temporal patterns of the wind, aiding in the calibration and validation of prediction models and the optimization of wind farms.

Figure 8 presents the Taylor Diagrams for heights of 100 and 150 m for the EMA Ilhéus locality. This type of diagram is a powerful tool for evaluating the performance of simulation models by comparing the statistics of standard deviation, correlation, and normalized RMSE between the simulations and the observations.

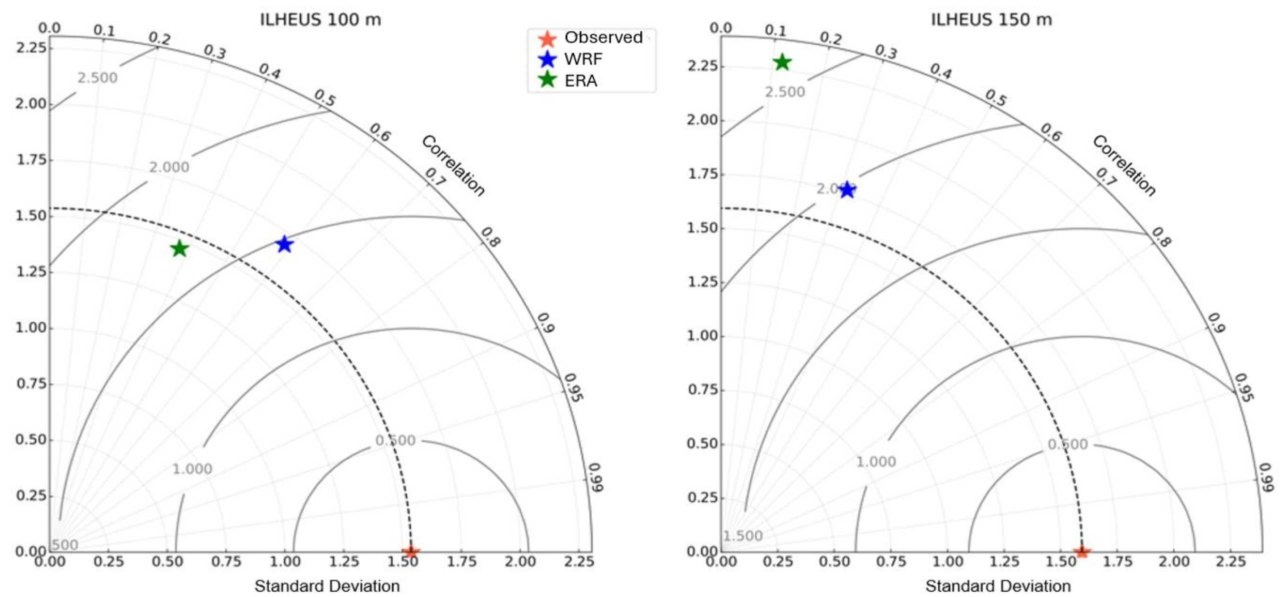

Figure 8 - Taylor Diagram for Observed and Simulated Data by ERA and WRF for EMA Ilhéus at 100 m and 150 m.

In the context of Ilhéus, at 100 m, the WRF model is close to the observed data but shows a slightly higher standard deviation. On the other hand, ERA5 has a lower standard deviation but is further from the observed data, indicating lower correlation. At 150 m, WRF remains close to the observed data, with a higher standard deviation but still good correspondence. In contrast, ERA5 shows a lower standard deviation but again is further from the observed data.

Analyzing the WRF model data for an altitude of 100 m, it is noted that the wind speed for the Ilhéus region has correlations of 0.6, suggesting lower simulation accuracy. This lower correlation observed in Ilhéus may be associated with the specific topography and roughness of the analyzed area.

Overall, at 100 m height, a low correlation was observed in the ERA5 data, where the measurement point showed the lowest correlation, with a value of 0.4, indicating a less accurate correspondence with the observed data.

At the height of 150 m, on the radial axis, the standard deviation of the observed data is represented by the red star, serving as a reference. The blue star (WRF) shows a standard deviation close to 2.0, indicating a variation similar to that observed but with some discrepancies. The green star (ERA) shows a larger standard deviation, close to 2.5, indicating greater variability in the simulated data. The correlation is represented by concentric contour lines, where the blue star (WRF) has a high correlation, close to 0.95, suggesting strong agreement with the temporal pattern of the observed data. The green star (ERA) has a slightly lower correlation, around 0.85.

The dashed lines represent the normalized RMSE, combining standard deviation and correlation for an overall measure of model accuracy. The RMSE for WRF is relatively low, indicating that the model captures the characteristics of the observed data well, while the RMSE for ERA is higher, reflecting discrepancies observed in standard deviation and correlation.

The analysis reveals that the WRF model has greater accuracy in simulating wind speeds at 150 m in the Ilhéus locality compared to the ERA model. Although both models show good correlation with the observational data, WRF has a standard deviation closer to the observed and a lower RMSE, indicating a better representation of wind conditions. These results are consistent with studies that highlight the importance of validating wind simulation models. Teng and Markfort (2020) emphasize the need to calibrate models with local data to improve the accuracy of wind forecasts. Barber et al. (2022) discusses how quantitative performance assessment of models, using statistics such as standard deviation and correlation, is crucial to ensure the reliability of simulated data.

Average Wind Speeds from the WRF Model for the Study Region

The modeling results were organized for heights of 100 m and 150 m, allowing for a more comprehensive analysis.

These analyses were conducted by grouping the results by annual periods and seasons, aiming to capture relevant nuances for understanding wind patterns in the studied region.

Seasonal Analysis

The analysis of average wind speeds by season allows the identification of seasonal variations in the region's wind patterns. The map is subdivided to represent Spring, Summer, Autumn, and Winter, highlighting specific trends and anomalies for each season. This approach provides essential data to understand the variation of wind speeds throughout the year.

Figures 9 and 10 display the wind speed information over the study period for the heights of 100 and 150 m, respectively, organized by season.

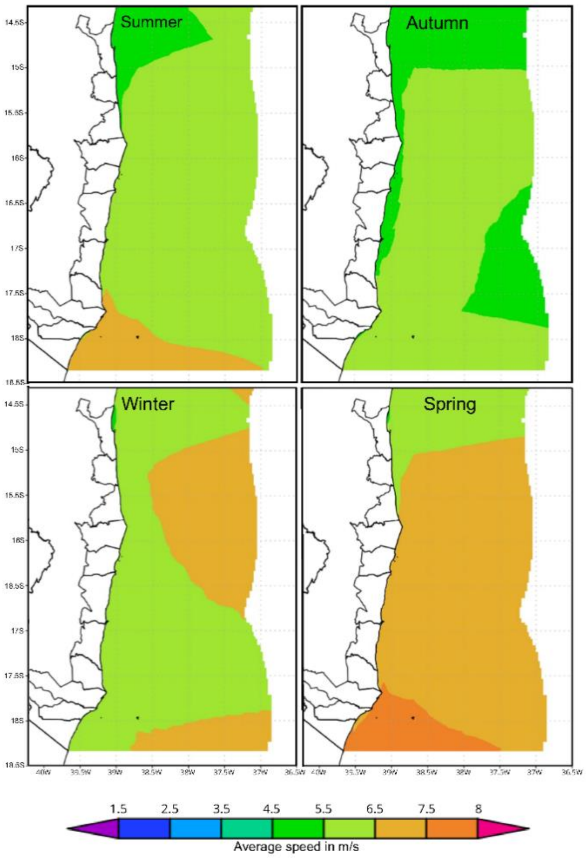

Figure 9 - Seasonal Average Speed at 100m Height.

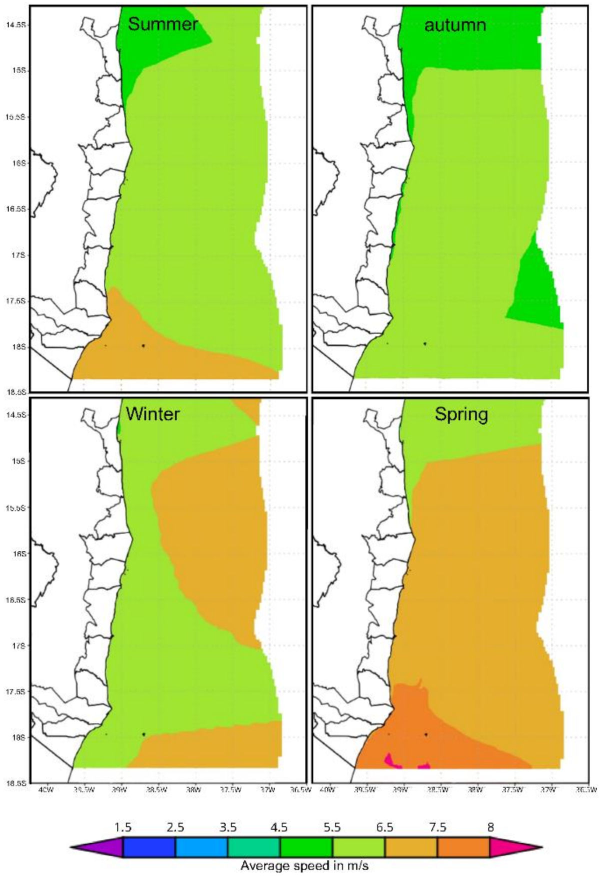

Figure 10 - Seasonal Average Speed at 150m Height.

In Figure 9, which presents the wind speeds at 100 m height, significant variations are observed throughout the seasons. During summer, wind speeds are lower in the south of the study area, ranging between 1.5 and 3.5 m/s around latitude 18.5°S. In contrast, to the north, near 14.5°S, speeds are slightly higher, reaching between 3.5 and 4.5 m/s. This pattern indicates a slight intensification of winds along the northern coast during summer. In autumn, the distribution of wind speeds becomes more uniform along the coast, with most of the region showing speeds between 3.5 and 4.5 m/s, while small areas around 14.5°S show slightly higher speeds, between 4.5 and 5.5 m/s.

In winter, there is an intensification of winds in the interior and south of the study area, with speeds predominantly between 4.5 and 5.5 m/s at latitudes close to 17.5°S and 18.5°S. In contrast, coastal areas between 14.5°S and 16°S show lower speeds, ranging between 3.5 and 4.5 m/s, evidencing a significant seasonal pattern in which winter brings stronger winds to the south. During spring, an increase in wind speeds is observed in the southern part of the study area, with averages up to 5.5 m/s, particularly around 18°S. At the same time, the center and north, between 14.5°S and 16.5°S, maintain a distribution of speeds between 3.5 and 4.5 m/s, similar to that observed in autumn, but with larger areas in the south reaching higher speeds.

Figure 10, which illustrates wind speeds at 150 m height, reveals that average speeds are generally higher than those observed at 100 m. In summer, most of the region presents speeds between 3.5 and 4.5 m/s, with the coastal area around 14.5°S showing more intense winds, between 4.5 and 5.5 m/s. In autumn, the distribution of wind speeds remains similar to summer, but with a slight overall intensification, especially in regions between 14.5°S and 16°S, where speeds range between 4.5 and 5.5 m/s. This suggests seasonal consistency in stronger winds at this height.

During winter, the region shows stronger winds in the south and central part, with speeds varying between 5.5 and 6.5 m/s in areas near 18°S and 17.5°S. In contrast, areas to the north, around 14.5°S to 16°S, show a slight reduction, with speeds predominantly between 4.5 and 5.5 m/s, highlighting the seasonal intensification of winds in the south. In spring, the pattern of stronger winds in the south continues, with speeds up to 6.5 m/s around 18.5°S, while in the northern areas, between 14.5°S and 16°S, a slight reduction is observed. Speeds between 4.5 and 5.5 m/s dominate most of the region, similar to winter, but with a trend toward higher intensities in the south.

Comparing Figures 9 and 10, it is evident that height has a significant impact on wind speed intensity. Generally, speeds increase with height, and seasonal variations are more pronounced at 150 m. This suggests that height is a crucial factor in wind intensification, and this information is essential for planning and optimizing offshore wind projects in the region. Especially during winter and spring, stronger winds occur in the south, indicating potential preferential sites for wind farm installations. These analyses help to better understand how seasonal patterns and height affect wind speed, providing valuable insights for the development of renewable energy in the coastal region between 14.5°S and 18.5°S in the state of Bahia.

Annual Analysis

Figure 11 displays the annual average wind speed information for the heights of 100 and 150 m, respectively.

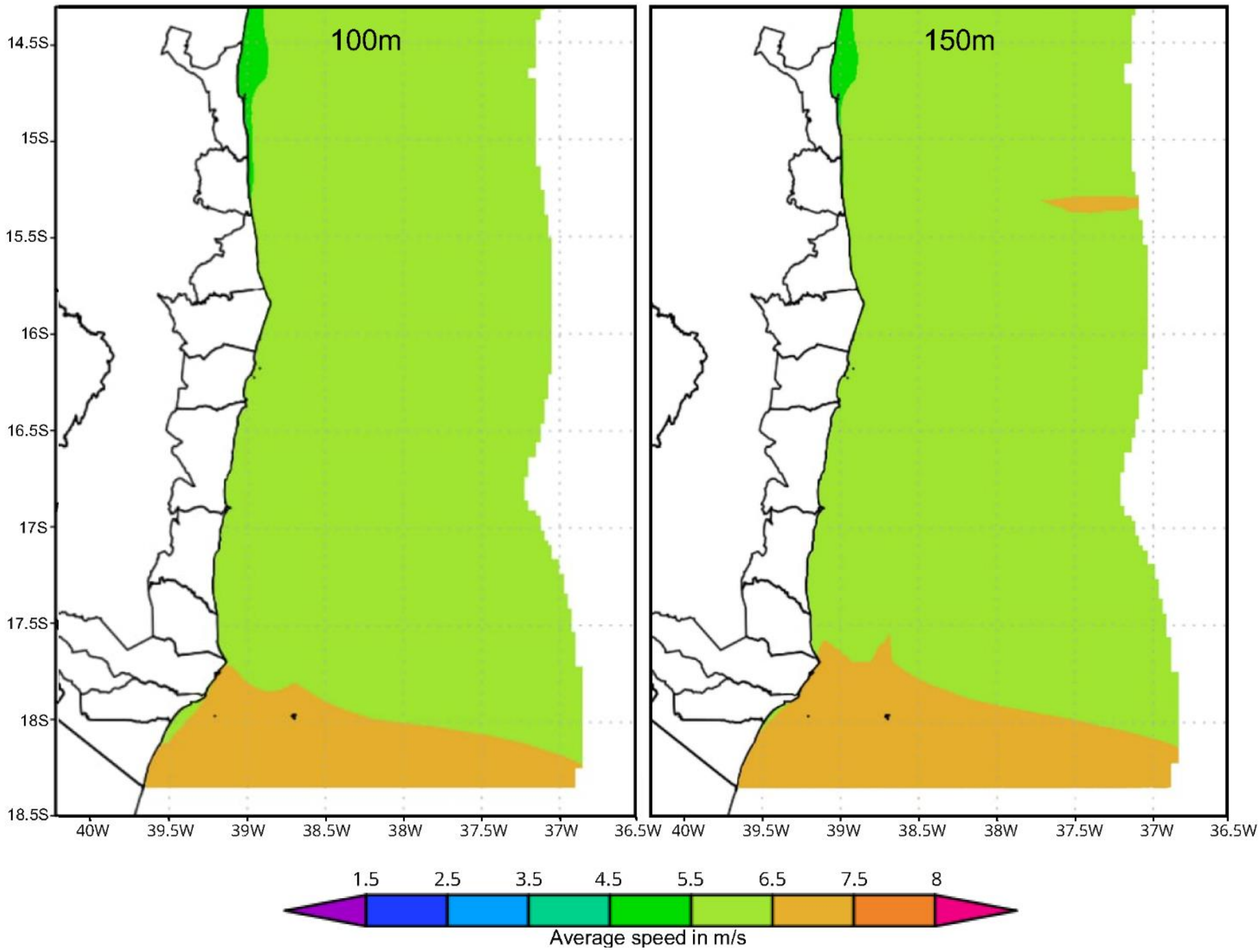

Figure 11 - Annual Average Speed for Heights of 100 m and 150 m.

At 100 m height, the analysis in Figure 11 reveals that wind speeds are predominantly moderate along the coast, with most of the area presenting average speeds between 3.5 and 4.5 m/s. The regions around 17.5°S to 18.5°S and southwest show higher speeds, ranging from 4.5 to 5.5 m/s. This distribution suggests that areas around these latitudes are more prone to stronger winds, which can be favorable for wind energy generation (Pimenta et al., 2019). Areas near the coast between 14.5°S and 16°S exhibit slightly lower speeds, ranging between 3.5 and 4.5 m/s, indicating lower wind intensity compared to the southern latitudes.

At 150 m height, Figure 11 shows a general increase in wind speeds across the region. Most of the area presents speeds between 4.5 and 5.5 m/s, with some regions around 17.5°S to 18.5°S and offshore exhibiting even higher speeds, reaching up to 6.5 m/s. This pattern reflects an increase in wind intensity with altitude, especially in areas near these latitudes and in regions further from the coast. This increase in wind speed with height is consistent with the expected behavior due to the vertical wind profile, where speeds tend to increase as the distance from the Earth's surface increases.

Comparing the two heights, it is clear that the coastal region between 17.5°S and 18.5°S in the state of Bahia presents significant potential for the development of wind projects, especially when considering the installation of taller turbines that can capture stronger winds (Pimenta et al., 2019). The difference in average speeds between 100 m and 150 m highlights the importance of height selection in optimizing the efficiency of wind energy projects.

The analysis of annual average wind speeds, as shown in Figure 11, provides valuable insights into the spatial and vertical distribution of wind intensity in the region. This information is essential for strategic decision-making in selecting sites for wind turbine installations, maximizing the utilization of available wind resources. The areas around 17.5°S to 18.5°S in the coastal region of Bahia emerge as the most promising sites for wind energy exploration, benefiting from stronger and more consistent winds throughout the year.

Conclusions

This study investigated the offshore wind potential in the coastal region of southern Bahia, highlighting seasonal variations in wind speeds, validating numerical models (WRF and ERA5), and providing technical support for the strategic planning of wind energy projects. The main topics addressed throughout the study included the characterization of the wind profile, the analysis of the most favorable seasons, and the importance of model validation for accurate estimates.

The research revealed that wind speeds in the region exhibit significant seasonal variations. During the summer, winds are weaker, especially near latitude 18.5°S, with speeds ranging from 1.5 to 3.5 m/s at 100 m altitude. In contrast, winter showed intensified wind speeds, reaching between 4.5 and 5.5 m/s, particularly between latitudes 17.5°S and 18.5°S. These findings confirm winter as the most favorable season for wind energy generation.

Additionally, the analysis revealed that wind speeds increase with altitude. At 150 m, wind speeds ranged between 4.5 and 5.5 m/s, with peaks of up to 6.5 m/s, highlighting the importance of turbines installed at higher altitudes to maximize energy efficiency. This finding corroborates the relevance of using validated models to identify ideal conditions for offshore projects.

The validation of the WRF and ERA5 models using data from the Ilhéus Automatic Weather Station demonstrated good overall agreement, despite minor discrepancies. While ERA5 underestimated wind speeds in the afternoon, WRF showed underestimations at specific times. These results confirm the reliability of the models, reinforcing their utility for future studies on offshore wind potential.

The results confirmed the objectives outlined at the beginning of the study: average wind speeds were estimated, the WRF and ERA5 models were validated, and a solid technical foundation was established for the strategic planning of wind energy projects. However, to improve understanding and reduce uncertainties, it is recommended that future studies extend the analysis period and integrate observational data from locations further offshore. Additionally, assessments of economic feasibility and environmental impacts could further enhance the practical applicability of the findings.

With these results, this study contributes to the advancement of renewable energy research in Brazil, demonstrating the high potential of the southern Bahia region for offshore wind energy projects. This research provides a robust technical framework to support strategic decision-making and reinforces the relevance of using numerical tools in wind studies.

Acknowledgments

The authors are grateful to the faculty of the Programa de Pós-Graduação em Ciências e Tecnologias Ambientais – PPGCTA/UFSB/IFBA and the Programa de Pós-Graduação em Engenharia Industrial – PEI/UFBA. We also acknowledge the support provided by Edital nº 25/2023/PRPGI/IFBA of September 12, 2023.

References

Alayat, M., Kassem, Y., & Çamur, H. (2018). Assessment of wind energy potential as a power generation source: A case study of eight selected locations in Northern Cyprus. *Energies*, *11*(10), 2697. https://doi.org/10.3390/en11102697

Anacona, H. V., et al. (2023). Wind simulations over Western Patagonia using the Weather Research and Forecasting model and reanalysis. *Atmosphere, 14*(7), 1062. https://doi.org/10.3390/atmos14071062

Andrade, A. R. de et al. (2021). Wind speed trends and the potential of electricity generation at new wind power plants in Northeast Brazil. *Journal of the Brazilian Society of Mechanical Sciences and Engineering, 43*(4), 182. http://dx.doi.org/10.1007/s40430-021-02911-y

Araújo, R. D., & Gorayeb, A. (2023). Perception of the socio-environmental impacts caused by wind generators in the state of Piauí, Northeast of Brazil. *Sustainability in Debate, 14*(3), 52–87. http://dx.doi.org/10.18472/SustDeb.v14n3.2023.50457

Bahamonde, M. I., & Litrán, S. P. (2019). Study of the energy production of a wind turbine in the open sea considering the continuous variations of the atmospheric stability and the sea surface roughness. *Renewable Energy, 135*, 163–175. https://doi.org/10.1016/j.renene.2018.11.075

Bañuelos-Ruedas, F., Angeles-Camacho, C., & Rios-Marcuello, S. (2010). Analysis and validation of the methodology used in the extrapolation of wind speed data at different heights. *Renewable and Sustainable Energy Reviews, 14*(8), 2383–2391. https://doi.org/10.1016/j.rser.2010.05.001

Barber, S., et al. (2022). The wide range of factors contributing to wind resource assessment accuracy in complex terrain. *Wind Energy Science, 7*(4), 1503–1525. https://doi.org/10.5194/wes-7-1503-2022

Barroso, L. L., et al. (2022). Aspectos gerais sobre a viabilidade de instalação de energia eólica no Brasil. *Research, Society and Development, 11*(9), e308911931781. http://dx.doi.org/10.33448/rsd-v11i9.31781

Barthelmie, R. J., Wang, H., Doubrawa, P., & Pryor, S. C. (2016). *Best practice for measuring wind speeds and turbulence offshore through in-situ and remote sensing technologies*. Departamento de Energia dos Estados Unidos. https://doi.org/10.7298/X4QV3JGF

Benesty, J., Chen, J., Huang, Y., & Cohen, I. (2009). Pearson correlation coefficient. In *Noise reduction in speech processing* (pp. 37-40). Springer. https://doi.org/10.1007/978-3-642-00296-0_5

Brower, M. (2012). *Wind resource assessment: A practical guide to developing a wind project.* John Wiley & Sons. https://doi.org/10.1002/9781118249864

Carvalho, D., Rocha, A., Gómez-Gesteira, M., & Santos, C. S. (2014). Comparison of reanalyzed, analyzed, satellite-retrieved and NWP modelled winds with buoy data along the Iberian Peninsula coast. *Remote Sensing of Environment, 152*, 480–492. https://doi.org/10.1016/j.rse.2014.07.017

Carvalho, D., Rocha, A., Gómez-Gesteira, M., & Santos, C. S. (2014). Sensitivity of the WRF model wind simulation and wind energy production estimates to planetary boundary layer parameterizations for onshore and offshore areas in the Iberian Peninsula. *Applied Energy, 135*, 234–246. https://doi.org/10.1016/j.apenergy.2014.08.086

Centro de Pesquisas de Energia Elétrica - CEPEL. (2017). *Atlas do potencial eólico brasileiro: Simulações 2013* (1ª ed.). CEPEL. Disponível em http://mtc-m21b.sid.inpe.br/col/sid.inpe.br/mtc-m21b/2017/12.21.11.22/doc/Novo-Atlas-do-Potencial-Eolico-Brasileiro-SIM_2013.pdf

Chancham, C., Waewsak, J., & Gagnon, Y. (2017). Offshore wind resource assessment and wind power plant optimization in the Gulf of Thailand. *Energy, 139*, 706–731. DOI: 10.1016/j.energy.2017.08.026

Coles, S. (2001). *An introduction to statistical modeling of extreme values* (1st ed.). Springer London. https://doi.org/10.1007/978-1-4471-3675-0

Coriolano, T. R., et al. (2022). Study of the temporal variation of offshore wind energy potential in southeast Brazil. *Ciência e Natura, 44*. http://dx.doi.org/10.5902/2179460X68814

Crippa, P., et al. (2021). A temporal model for vertical extrapolation of wind speed and wind energy assessment. *Applied Energy, 301*, 117378. https://doi.org/10.1016/j.apenergy.2021.117378

Daley, R. (1991). *Atmospheric data analysis*. Cambridge University Press. https://doi.org/10.1002/joc.3370120708

de Jong, P., et al. (2017). Forecasting high proportions of wind energy supplying the Brazilian Northeast electricity grid. *Applied Energy, 195*, 538–555. https://doi.org/10.1016/j.apenergy.2017.03.058

Lucena, A. F. P., Szklo, A. S., Schaeffer, R., & Dutra, R. M. (2010). The vulnerability of wind power to climate change in Brazil. *Renewable Energy*, *35*(5), 904–912. https://doi.org/10.1016/j.renene.2009.10.022

Delgado, F., & Filgueiras, R. (2022). O&G e energia renovável offshore: perspectivas e desafios. *Revista Conjuntura Econômica, 76*, 42–44.

Dörenkämper, M., et al. (2020). The making of the New European Wind Atlas – Part 2: Production and evaluation. *Geoscientific Model Development, 13*(10), 5079–5102. https://doi.org/10.5194/gmd-13-5079-2020

Franz, G., et al. (2021). Coastal ocean observing and modeling systems in Brazil: Initiatives and future perspectives. *Frontiers in Marine Science, 8*. https://doi.org/10.3389/fmars.2021.681619

Freire, A. Í., & Fontgalland, I. L. (2022). Perspectivas e desafios econômicos da geração de energia eólica na região Nordeste do Brasil. *Research, Society and Development, 11*(1), e58911125429. https://doi.org/10.33448/rsd-v11i1.25429

Freire, L. S. (2022). Large-eddy simulation of the atmospheric boundary layer with near-wall resolved turbulence. *Boundary-Layer Meteorology, 184*(1), 25–43. https://doi.org/10.1007/s10546-022-00702-z

Góes, M. de F. B., et al. (2021). Wind power projects in Brazil: Challenges and opportunities increasing co-benefits and implications for climate and energy policies. *Environment, Development and Sustainability, 23*(10), 15341–15367. https://doi.org/10.1007/s10668-021-01300-8

Golbazi, M., & Archer, C. L. (2020). Surface roughness for offshore wind energy. *Journal of Physics: Conference Series, 1452*(1), 012024. DOI: 10.1088/1742-6596/1452/1/012024

Gonçalves, L. de J. M., et al. (2024). Evaluation of a high-resolution WRF model for southeast Brazilian coast: The importance of physical parameterization to wind representation. *Atmosphere*, *15*(5), 533. https://doi.org/10.3390/atmos15050533

González-Mingueza, C., & Muñoz-Gutiérrez, F. (2014). RETRACTED: Wind prediction using Weather Research Forecasting model (WRF): A case study in Peru. *Energy Conversion and Management*, *81*, 363–373. https://doi.org/10.1016/j.enconman.2014.02.024

Gorayeb, A., Araújo, R. M., & Silva, C. F. (2022). Análise multicritério de parques eólicos onshore e offshore no Ceará: Em foco as comunidades tradicionais litorâneas. *Revista Mutirõ: Folhetim de Geografias Agrárias do Sul*, *3*(2), 32. https://doi.org/10.51359/2675-3472.2022.253079

Gorayeb, A., & Brannstrom, C. (2016). Toward participatory management of renewable energy resources (wind-farm) in Northeastern Brazil. *Mercator*, *15*(1), 105–115. DOI 10.4215/RM0000.0000.0000

Gorayeb, A., & Brannstrom, C. (2016). Toward participatory management of renewable energy resources (wind-farm) in northeastern Brazil. *Mercator*, *15*(1), 105–115. DOI: 10.4215/rm2016.1501.0008

Hersbach, H., et al. (2020). The ERA5 global reanalysis. *Quarterly Journal of the Royal Meteorological Society, 146*(730), 1999–2049. https://doi.org/10.1002/qj.3803

Jacondino, W. D., et al. (2021). Hourly day-ahead wind power forecasting at two wind farms in northeast Brazil using WRF model. *Energy*, *230*, 120841. https://doi.org/10.1016/j.energy.2021.120841

Juárez, A. A., et al. (2014). Development of the wind power in Brazil: Political, social and technical issues. Renewable and Sustainable Energy Reviews, 39, 828–834. https://doi.org/10.1016/j.rser.2014.07.086

Kaiser-Weiss, A. K., Kaspar, F., Heene, V., & Fiedler, S. (2015). Comparison of regional and global reanalysis near-surface winds with station observations over Germany. *Advances in Science and Research*, *12*(1), 187–198. https://doi.org/10.5194/asr-12-187-2015

Kent, C. W., Grimmond, C. S. B., Gatey, D., & Barlow, J. F. (2018). Assessing methods to extrapolate the vertical wind-speed profile from surface observations in a city centre during strong winds. *Journal of Wind Engineering and Industrial Aerodynamics*, *173*, 100–111. https://doi.org/10.1016/j.jweia.2017.12.013

Khan, K. S., & Tariq, M. (2018). Wind resource assessment using SODAR and meteorological mast: A case study of Pakistan. *Renewable and Sustainable Energy Reviews*, *81*, 2443–2449. https://doi.org/10.1016/j.rser.2017.06.040

Kosovic, B., Haupt, S. E., Adriaansen, D., Alessandrini, S., & Sullivan, P. (2020). A comprehensive wind power forecasting system integrating artificial intelligence and numerical weather prediction. *Energies*, *13*(6), 1372. https://doi.org/10.3390/en13061372

Kovalski, M. L. (2023). *Variabilidade de alta frequência da velocidade do vento próximo à superfície no Nordeste do Brasil: Clima presente e* *tendências futuras* (Dissertação de mestrado, Universidade de São Paulo, Instituto de Astronomia, Geofísica e Ciências Atmosféricas).

Kruse, C., Del Vento, D., Montuoro, R., Lubin, M., & McMillan, S. (2013, August). Evaluation of WRF scaling to several thousand cores on the Yellowstone supercomputer. Em *Proceedings of the Front Range Consortium for Research Computing Conference* (Vol. 14). Boulder, CO, EUA.

Lange, B., Larsen, S., Højstrup, J., & Barthelmie, R. J. (2004). Importance of thermal effects and sea surface roughness for offshore wind resource assessment. *Journal of Wind Engineering and Industrial Aerodynamics, 92*(11), 959–988. https://doi.org/10.1016/j.jweia.2004.06.002

Langenberg, B., Janczyk, M., Koob, V., & Kliegl, R. (2022). A tutorial on using the paired t test for power calculations in repeated measures ANOVA with interactions. *Behavior Research Methods, 55*(5), 2467–2484. https://doi.org/10.3758/s13428-022-01902-8

Letcher, T. (Ed.). (2023). *Wind energy engineering: A handbook for onshore and offshore wind turbines*. Elsevier. https://doi.org/10.1016/C2021-0-00258-3

Li, H., Claremar, B., Wu, L., Hallgren, C., Körnich, H., Rutgersson, A., & Ivanell, S. (2021). A sensitivity study of the WRF model in offshore wind modeling over the Baltic Sea. *Geoscience Frontiers, 12*(6), 101229. https://doi.org/10.1016/j.gsf.2021.101229

Li, J., Wang, G., Li, Z., Yang, S., & Chong, W. T. (2020). A review on development of offshore wind energy conversion system. *International Journal of Energy Research, 44*(12), 9283–9297. https://doi.org/10.1002/er.5751

Lima, M. A., Mendes, L. F. R., Mothé, G. A., Linhares, F. G., & Soares, S. R. (2020). Renewable energy in reducing greenhouse gas emissions: Reaching the goals of the Paris agreement in Brazil. *Environmental Development, 33*, 100504. https://doi.org/10.1016/j.envdev.2020.100504

Li, Z., Wan, B., Duan, Z., He, Y., Yu, Y., & Chen, H. (2023). Evaluation of HY-2C and CFOSAT satellite retrieval offshore wind energy using Weather Research and Forecasting (WRF) simulations. *Remote Sensing*, 15(17), 4172. https://doi.org/10.3390/rs15174172

Liu, X., Xing, X., Kang, C. W., & Zhang, X. (2024). *Towards Offshore Wind Farm Design through Comprehensive Meteo-Oceanographic Analysis in Extreme Weather Conditions*. *Ocean and Polar Engineering*, 2024.

Loriato, A. G., Salvador, N., Loriato, A. A. B., & Andrade, M. F. (2018). Inventário de emissões com alta resolução para a região da Grande Vitória utilizando o sistema de modelagem integrada WRF-SMOKE-CMAQ. *Revista Brasileira de Meteorologia, 33*(3), 521–536. https://doi.org/10.1590/0102-77863330046

Lucena, J. de A. Y., & Lucena, K. Â. A. (2019). Wind energy in Brazil: An overview and perspectives under the triple bottom line. *Clean Energy, 3*(2), 69–84. https://doi.org/10.1093/ce/zkz001

Lumbreras, S., & Ramos, A. (2013). Offshore wind farm electrical design: A review. *Wind Energy, 16*(3), 459–473. https://doi.org/10.1002/we.1498

Machrafi, H. (Ed.). (2012). *Green energy and technology*. Bentham Science Publishers. https://doi.org/10.2174/97816080528511120101

Marinha do Brasil. (n.d.). *Limites Marítimos e LEPLAC*. Diretoria de Hidrografia e Navegação. Disponível em https://www.marinha.mil.br/dhn/?q=pt-br/node/168

Maslor, N. A., & Hasan, H. B. (2024, January 24). Analysis of daily maximum temperature and wind speed in Malaysia using repeated measures ANOVA. *AIP Conference Proceedings*. AIP Publishing. https://doi.org/10.1063/5.0192718

Mathos, K. P., Donnou, H. E. V., & Kouchadé, C. A. (2020). Vertical extrapolation of wind speeds under a neutral atmosphere and evaluation of the wind energy potential on different sites in Guinea. *American Journal of Energy Engineering, 8*(1), 9. https://doi.org/10.11648/j.ajee.20200801.12

Mattar, C., & Borvarán, D. (2016). Offshore wind power simulation by using WRF in the central coast of Chile. *Renewable Energy, 94*, 22–31. https://doi.org/10.1016/j.renene.2016.03.041

Miglietta, M. M., Zecchetto, S., & De Biasio, F. (2013). A comparison of WRF model simulations with SAR wind data in two case studies of orographic lee waves over the Eastern Mediterranean Sea. *Atmospheric Research, 120–121*, 127–146. https://doi.org/10.1016/j.atmosres.2012.09.017

Moreno, R., Arias, E., Cazorla, D., & Pardo, J. J. (2020). Analysis of a new MPI process distribution for the Weather Research and Forecasting (WRF) model. *Scientific Programming, 2020*, 8148373. https://doi.org/10.1155/2020/8148373

Mughal, M. O., Lynch, M., Yu, F., & McGann, B. (2017). Wind modelling, validation and sensitivity study using Weather Research and Forecasting model in complex terrain. *Environmental Modelling & Software, 90*, 107–125. https://doi.org/10.1016/j.envsoft.2017.01.020

Muhammad, L. N. (2023). Guidelines for repeated measures statistical analysis approaches with basic science research considerations. *Journal of Clinical Investigation, 133*(11). https://doi.org/10.1172/JCI171058

Nascimento, M. M. de S., Shadman, M., Silva, C., & Nascimento, J. (2022). Offshore wind and solar complementarity in Brazil: A theoretical and technical potential assessment. *Energy Conversion and Management, 270*, 116194. https://doi.org/10.1016/j.enconman.2022.116194

Nezhad, M. M., Neshat, M., & Groppi, D. (2021). A primary offshore wind farm site assessment using reanalysis data: A case study for Samothraki Island. *Renewable Energy, 172*, 667–679. https://doi.org/10.1016/j.renene.2021.03.089

Olaofe, Z. O. (2019). Quantification of the near-surface wind conditions of the African coast: A comparative approach (satellite, NCEP CFSR, and WRF-based). *Energy, 189*, 116232. https://doi.org/10.1016/j.energy.2019.116232

Paulino, S. R., et al. (2023). Conflitos socioambientais e a implantação de parques eólicos no Nordeste brasileiro. *Sustainability in Debate, 14*(3), 21–51. https://doi.org/10.20873/j.sustain.14.3.2023

Pelser, T., et al. (2024). Reviewing accuracy & reproducibility of large-scale wind resource assessments. *Advances in Applied Energy, 13*, 100158. https://doi.org/10.1016/j.adapen.2024.100158

Perini, N. B. P., et al. (2022). Wind mapping using the mesoscale WRF model in a tropical region of Brazil. *Energy, 240*, 122491. https://doi.org/10.1016/j.energy.2021.122491

Petersen, E. L. (2017). In search of the wind energy potential. *Journal of Renewable and Sustainable Energy, 9*(5). https://doi.org/10.1063/1.4995245

Piasecki, A., Jurasz, J., & Kies, A. (2019). Measurements and reanalysis data on wind speed and solar irradiation from energy generation perspectives at several locations in Poland. *SN Applied Sciences, 1*(8), 865. https://doi.org/10.1007/s42452-019-0909-x

Pimenta, F. M., et al. (2019). Brazil offshore wind resources and atmospheric surface layer stability. *Energies, 12*(21), 4195. https://doi.org/10.3390/en12214195

Placide, G., & Lollchund, M. R. (2024). An evaluation of the reliability of the Weather Research Forecasting (WRF) model in predicting wind data: A case study of Burundi. *BMC Environmental Science, 1*(1), 2. https://doi.org/10.1186/s44329-024-00001-7

Rabelo, D. R., de Araújo, L. F., Santos, M. A., & Souza, J. M. (2023). Generation of wind energy in the state of Bahia, Brazil: Challenges and possibilities. *Revista Brasileira de Geografia Física, 16*(3), 1145–1155. https://doi.org/10.26848/rbgf.v16.3.p1145-1155

Saadatabadi, A. R., Mohammadi, H., & Asadi, F. (2024). Optimization and evaluation of the Weather Research and Forecasting (WRF) model for wind energy resource assessment and mapping in Iran. *Applied Sciences, 14*(8), 3304. https://doi.org/10.3390/app14083304

Sampaio, K. R. A., & Batista, V. (2021). O atual cenário da produção de energia eólica no Brasil: Uma revisão de literatura. *Research, Society and Development, 10*(1), e57710112107. https://doi.org/10.33448/rsd-v10i1.12107

Santana, L. V. R., Stosic, T., & Ferreira, T. A. E. (2020). Comparison of wind speed data in the Northeast of Brazil from ERA-40 and the National Institute of Meteorology (INMET) using entropy measurements. *Research, Society and Development, 9*(8), e446985257. https://doi.org/10.33448/rsd-v9i8.5257

Santana, L. V. R., & Silva, A. S. A. da. (2020). Análise de agrupamento da velocidade do vento no Nordeste do Brasil. Em *Ciências Exatas e da Terra: Exploração e Qualificação de Diferentes Tecnologias 2* (pp. 61–69). Atena Editora. DOI: 10.22533/at.ed.8562027105

Santos, J. V. C. (2020). *Estudo das características espaciais e temporais da velocidade do vento utilizando a técnica DFA e o modelo WRF em regiões do Estado da Bahia e no Oceano Atlântico Sul* (Tese de doutorado, Centro Universitário SENAI CIMATEC, Programa de Pós-Graduação em Modelagem Computacional e Tecnologia Industrial). Salvador: SENAI CIMATEC.

Sheridan, L. M., Phillips, C., Orrell, A. C., & Lantz, K. (2022). Validation of wind resource and energy production simulations for small wind turbines in the United States. *Wind Energy Science, 7*(2), 659–676. https://doi.org/10.5194/wes-7-659-2022

Shi, P., Leung, L. R., & Wang, B. (2024). *Development and evaluation of a new 4DEnVar-based weakly coupled ocean data assimilation system in E3SMv2*. Geoscientific Model Development. https://doi.org/10.5194/gmd-2024-183

Silva, G. K. da, Santos, A. C. dos, Silva, M. V. M. da, & Lima, J. S. (2017). Estudo dos padrões de ventos offshore no litoral do Ceará utilizando dados estimados pelo produto de satélites BSW. *Revista Brasileira de Meteorologia, 32*(4), 679–690. https://doi.org/10.1590/0102-77863240013

Silva, S. S. F. da, Alves, A. C., & Ramalho, Â. M. C. (2020). Energia eólica e complementaridade energética: Estratégia e desafio para o desenvolvimento sustentável na região Nordeste do Brasil. *Qualitas Revista Eletrônica, 19*(3), 53. http://dx.doi.org/10.18391/req.v19i3.5640

Silva, S. S. F. da, & Cândido, G. A. (2015). Energy matrix clean and renewable: A challenge for the National energy planning and an opportunity for the Northeast Region of Brazil. *Revista Espacios, 36*(15). DOI: 10.48082/espacios-a24v45n05

Silveira, W. W. da, & Carvalho, V. S. B. (2021). Avaliação das condições meteorológicas simuladas pelo modelo WRF na região metropolitana do Rio de Janeiro em dias com altas concentrações de poluentes. *Revista Brasileira de Meteorologia, 36*(2), 317–325. https://doi.org/10.1590/0102-77863623005

Simas, M., & Pacca, S. (2014). Assessing employment in renewable energy technologies: A case study for wind power in Brazil. *Renewable and Sustainable Energy Reviews, 31*, 83–90. https://doi.org/10.1016/j.rser.2013.11.046

Stoevesandt, B., Schepers, J. G., Martínez-Tossas, L. A., & Le Pape, A. (Eds.). (2022). *Handbook of wind energy aerodynamics*. Springer Nature. https://doi.org/10.1007/978-3-030-31307-4

Stull, R. (2016). *Practical meteorology: An algebra-based survey of atmospheric science* (Edição ilustrada). AVP International, University of British Columbia, BC Open Textbook Collection.

Teng, J., & Markfort, C. D. (2020). A calibration procedure for an analytical wake model using wind farm operational data. *Energies, 13*(14), 3537. http://dx.doi.org/10.3390/en13143537

Tian, X., Conibear, L., & Steward, J. (2023). A neural-network based MPAS—Shallow water model and its 4D-Var data assimilation system. *Atmosphere, 14*(1), 157. https://doi.org/10.3390/atmos14010157

Tuchtenhagen, P., et al. (2020). WRF model assessment for wind intensity and power density simulation in the southern coast of Brazil. *Energy, 190*, 116341. http://dx.doi.org/10.1016/j.energy.2019.116341

Tuchtenhagen, P., Basso, J., & Yamasaki, Y. (2014). Avaliação do p otencial eólico no Brasil em 2011. *Ciência e Natura, 36*(2). http://dx.doi.org/10.5902/2179460X13148

Tuchtenhagen, P. N. (2019). *Variabilidade do vento e potencial para energia eólica offshore no litoral sul do Brasil* (Tese de doutorado). Universidade Federal do Rio Grande do Norte, Centro de Ciências Exatas e da Terra, Programa de Pós-Graduação em Ciências Climáticas, Natal.

Turkovska, O., Castro, G., Klingler, M., Gomes, S. C., & Lucena, A. F. P. (2021). Land-use impacts of Brazilian wind power expansion. *Environmental Research Letters, 16*(2), 024010. https://doi.org/10.1088/1748-9326/abd12f

Ulazia, A., Saenz, J., & Ibarra-Berastegui, G. (2016). Sensitivity to the use of 3DVAR data assimilation in a mesoscale model for estimating offshore wind energy potential: A case study of the Iberian northern coastline. *Applied Energy, 180*, 617–627. https://doi.org/10.1016/j.apenergy.2016.07.115

Varga, Á. J., & Breuer, H. (2022). Evaluation of convective parameters derived from pressure level and native ERA5 data and different resolution WRF climate simulations over Central Europe. *Climate Dynamics, 58*(5–6), 1569–1585. https://doi.org/10.1007/s00382-021-05979-3

Vidal, D. B., Torres, E. A., & de Jong, P. (2023). Study of indicators on regulation for offshore wind energy exploitation in Brazil. *Delos: Desarrollo Local Sostenible, 16*(48), 3375–3398. https://doi.org/10.55905/rdelosv16.n48-025

Vinhoza, A., & Schaeffer, R. (2021). Brazil's offshore wind energy potential assessment based on a spatial multi-criteria decision analysis. *Renewable and Sustainable Energy Reviews, 146*, 111185. https://doi.org/10.1016/j.rser.2021.111185

Wang, Y., Li, X., & Chen, Y. (2023). Combined assimilation of hourly rainfall data and every 10-min AHI radiance with WRF 4DVar for the short-range heavy rainfall forecast in Eastern China. *Atmospheric Research, 292*(1), 106867. https://doi.org/10.1016/j.atmosres.2023.106867

Wieringa, J. (1986). Roughness-dependent geographical interpolation of surface wind speed averages. Quarterly Journal of the Royal Meteorological Society, 112(473), 867–889. https://doi.org/10.1002/qj.49711247316

Wilks, D. S. (2020). *Statistical methods in the atmospheric sciences* (4ª ed.). Elsevier. https://doi.org/10.1016/C2017-0-03921-6

Willmott, C. J., Matsuura, K., & Robeson, S. M. (2009). Ambiguities inherent in sums-of-squares-based error statistics. *Atmospheric Environment*, *43*(3), 749–752. https://doi.org/10.1016/j.atmosenv.2008.10.005

Witha, B., Hahmann, A. N., Sile, T., Dörenkämper, M., Ezber, Y., Bustamante, E. G., Gonzalez-Rouco, J. F., Leroy, G., & Navarro, J. (2019). *Report on WRF model sensitivity studies and specifications for the mesoscale wind atlas production runs: Deliverable D4.3*. NEWA - New European Wind Atlas. https://doi.org/10.5281/zenodo.2682604

Wu, C., Wang, Q., Luo, K., & Fan, J. (2022). Mesoscale impact of the sea surface on the performance of offshore wind farms. *Journal of Cleaner Production*, *372*, 133741. https://doi.org/10.1016/j.jclepro.2022.133741

Xiang, L., Yang, X., Hu, A., Su, H., & Wang, P. (2022). Condition monitoring and anomaly detection of wind turbine based on cascaded and bidirectional deep learning networks. *Applied Energy*, *305*, 117925. https://doi.org/10.1016/j.apenergy.2021.117925

Yu, E., Bai, R., Chen, X., & Shao, L. (2022). Impact of physical parameterizations on wind simulation with WRF V3.9.1.1 under stable conditions at planetary boundary layer gray-zone resolution: A case study over the coastal regions of North China. Geoscientific Model Development, 15(21), 8111–8134. https://doi.org/10.5194/gmd-15-8111-2022

Zack, J., Natenberg, E., Young, S., Manobianco, J., & Kamath, C. (2010). *Application of ensemble sensitivity analysis to observation targeting for short-term wind speed forecasting* (LLNL-TR-424442). Lawrence Livermore National Laboratory. https://doi.org/10.2172/972845

Zucatelli, P. J., Nascimento, E. G. S., Santos, A. Á. B., Arce, A. M. G., & Lopes, F. C. (2021). An investigation on deep learning and wavelet transform to nowcast wind power and wind power ramp: A case study in Brazil and Uruguay. Energy, 230, 120842. https://doi.org/10.1016/j.energy.2021.120842